computation

MDPI

Article

Optimal Selection of Conductors in Three-Phase Distribution Networks Using a Discrete Version of the Vortex Search Algorithm

John Fernando Martínez-Gil [1], Nicolas Alejandro Moyano-García [1], Oscar Danilo Montoya [2,3,*] and Jorge Alexander Alarcon-Villamil [2]

[1] Ingeniería Eléctrica, Universidad Distrital Francisco José de Caldas, Bogotá D.C. 110231, Colombia; jofmartinezg@correo.udistrital.edu.co (J.F.M.-G.); namoyanog@correo.udistrital.edu.co (N.A.M.-G.)
[2] Facultad de Ingeniería, Universidad Distrital Francisco José de Caldas, Bogotá D.C. 110231, Colombia; jaalarconv@udistrital.edu.co
[3] Laboratorio Inteligente de Energía, Universidad Tecnológica de Bolívar, Cartagena 131001, Colombia
* Correspondence: odmontoyag@udistrital.edu.co

Abstract: In this study, a new methodology is proposed to perform optimal selection of conductors in three-phase distribution networks through a discrete version of the metaheuristic method of vortex search. To represent the problem, a single-objective mathematical model with a mixed-integer nonlinear programming (MINLP) structure is used. As an objective function, minimization of the investment costs in conductors together with the technical losses of the network for a study period of one year is considered. Additionally, the model will be implemented in balanced and unbalanced test systems and with variations in the connection of their loads, i.e., Δ- and *Y*-connections. To evaluate the costs of the energy losses, a classical backward/forward three-phase power-flow method is implemented. Two test systems used in the specialized literature were employed, which comprise 8 and 27 nodes with radial structures in medium voltage levels. All computational implementations were developed in the MATLAB programming environment, and all results were evaluated in DigSILENT software to verify the effectiveness and the proposed three-phase unbalanced power-flow method. Comparative analyses with classical and Chu & Beasley genetic algorithms, tabu search algorithm, and exact MINLP approaches demonstrate the efficiency of the proposed optimization approach regarding the final value of the objective function.

Keywords: conductor selection; mathematical optimization; distribution systems; three-phase; power flow; energy losses; vortex search algorithm

check for updates

Citation: Martínez-Gil, J.F.; Moyano-Garcia, N.A.; Montoya, O.D.; Alarcon-Villamil, J.A. Optimal Selection of Conductors in Three-Phase Distribution Networks Using a Discrete Version of the Vortex Search Algorithm. *Computation* **2021**, *9*, 80. https://doi.org/10.3390/computation9070080

Academic Editors: George Tsakalidis and Kostas Vergidis

Received: 22 May 2021
Accepted: 16 July 2021
Published: 18 July 2021

Publisher's Note: MDPI stays neutral with regard to jurisdictional claims in published maps and institutional affiliations.

Copyright: © 2021 by the authors. Licensee MDPI, Basel, Switzerland. This article is an open access article distributed under the terms and conditions of the Creative Commons Attribution (CC BY) license (https://creativecommons.org/licenses/by/4.0/).

1. Introduction

Electrical distribution networks represent the largest portion of power systems (i.e., thousands of kilometers of length) entrusted with distributing electrical services to end-users via medium- and low- voltage levels by interfacing transmission/sub-transmission grids with consumers in rural and urban areas [1,2]. The main characteristics of these grids are as follows: (i) a radial configuration reduces the investment and operation costs as well as simplifies the coordination scheme of the protective devices [3]; (ii) the constructive structure of the network, i.e., horizontal and vertical configurations, ensures that the line impedances are unbalanced [4]; and (iii) the nature of the loads is unbalanced with Δ- and *Y*-connections [5]. Because of these characteristics in the configuration of the distribution systems, necessary efficient methodologies are required to plan these grids to ensure their correct operation with minimum investment and operative costs for a planning horizon [6]. For the optimal design of electrical distribution networks, multiple aspects must be considered including construction of new substations to increase the capability of the existing ones, changing calibers of the conductors in the existing

distribution lines, selecting calibers for new routes, and minimizing operational costs regarding energy losses [7]. To contribute in part to the general planning optimization model for optimal planning of electrical distribution networks, in this research, we explore the problem of optimal selection of conductors in three-phase balanced and unbalanced distribution networks, where the topology of the network is considered fixed by the distribution company in a previous design step [8]. Even if the optimal selection of the conductors in electrical distribution networks is a sub-problem in the general planning of the distribution systems, this is a complex problem to solve because it is represented by a mixed-integer nonlinear programming (MINLP) model [9]. Note that this problem is binary (also integer) in relation to the selection of a particular caliber for each route and nonlinear due to the three-phase power balance equations [5].

To solve this MINLP model, studies have proposed multiple optimization approaches, some of which are presented below. Authors in [10] presented a tabu search algorithm to select calibers in three-phase balanced networks composed of 8 and 202 nodes. Two simulation scenarios were considered to evaluate the objective function (i.e., investment in conductors and energy loss costs); these scenarios correspond to the peak load demand during all hours of the year and three periods of time with demands of 100% (1000 h), 60% (6760 h), and 30% (1000 h). The numerical results demonstrate that the second scenario is more realistic and reduces the amount of investment in conductors with respect to the peak load case in which these are over-sized. In [11], the authors applied the sine-cosine algorithm to select calibers of the conductors in a real Egyptian distribution system considering 20 different caliber options. The results obtained highlighted the effectiveness of the proposed method in reducing the network losses while maintaining the specified constraints over a ten-year period, considering a high annual load growth rate. Authors of [12] analyzed a medium-voltage distribution network to reduce the inversion and operation costs through the optimal selection of routes from the main substations and their optimal calibers. As a solution, a constructive graph algorithm was used that works with a classical backward/forward method to evaluate the electrical variables of the network. The proposed methodology was tested in the 54-node test feeder; however, the authors did not provide comparisons with other methodologies to verify the efficiency of their proposed method. In [13], a methodology for selecting calibers in distribution networks with the salp swarm optimization is presented. The objective function considers the minimization of the annual energy loss costs and the total investment in conductors while complying with the system voltage limits and thermal capacities of the conductor. Numerical results in a real Egyptian test feeder demonstrated the effectiveness and robustness of the methodology when considering the penetration of distributed generation since these allow us to increase the system's hosting capacity.

A complete list of algorithms used to solve the problem of the optimal selection of calibers in distribution networks is provided in Table 1.

Table 1. Summary of methodologies used in the literature for optimal selection of calibers in distribution networks.

Solution Methodology	Reference	Year
Constructive heuristic algorithm	[12,14]	{2002, 2017}
Genetic algorithms	[9,15,16]	{2010, 2011, 2013, 2019}
Harmony search algorithm	[17]	2011
Non-dominated elitist sorting algorithm	[18]	2011
Particle swarm optimization	[19]	2012
Bacterial search algorithm	[20]	2015
Sine-cosine optimization algorithm	[11]	2017
Crow search algorithm	[21]	2017
Teaching-learning based optimization algorithm	[22]	2017
Tabu search algorithm	[10]	2018
Exact MINLP solution in GAMS	[23,24]	{2018, 2021}
Whale optimization algorithm	[25]	2019
Branch wise minimization technique	[26]	2019
Evaporation rate water cycle algorithm	[27]	2021

The main characteristic of the optimization (heuristic and exact) methods reported in Table 1 is that in a single-objective function formulation, all methodologies consider in the objective function the annualized investment costs of conductors in conjunction with the costs of the energy losses; in addition, the authors typically consider three-phase balanced grids which can be represented with a single-phase equivalent. However, unlike previous works, in this research, we propose the application of a discrete version of the vortex search algorithm (DVSA) to solve the problem of the optimal selection of calibers in three-phase balanced and unbalanced distribution grids. Note that the discrete version of the vortex search algorithm has only been proposed in two recent studies related to phase-balancing in three-phase radial grids [5] and optimal location of photovoltaic sources in single-phase distribution grids [28]. The main advantage of using the DVSA corresponds is its ability in exploring and exploiting the solution space via hyper-ellipses with a variable radius, which is generated with a normal Gaussian distribution around the best current solution, i.e., the center of the hyper-ellipse [29]. Numerical comparisons with classical methods such as the exact MINLP solution with the GAMS package, the tabu search algorithm, and the classical and improved genetic algorithms will demonstrate the effectiveness and robustness of the proposed optimization methodology. The main contributions of this research are presented below:

- The solution of the exact MINLP model for the problem of the optimal selection of calibers in three-phase balanced and unbalanced distribution networks using a master-slave optimization approach is proposed. The master stage corresponds to the discrete version of the vortex search algorithm which defines the set of calibers to be installed in all routes of the network. The slave stage is the three-phase unbalanced backward/forward power-flow method used to evaluate the operative costs of the network, including loads connected with Δ and/or Y structures.
- We evaluate the three different scenarios regarding the load consumption for the planning period to determine the optimal set of calibers that must be installed in the distribution network. These periods are (i) the load peak case during 8760 h (one ordinary year), (ii) three levels of consumption with values of 100% (1000 h), 60% (6760 h), and 30% (1000 h), and (iii) consumption with a typical load curve considering 24 h.
- A grid with unbalanced loads is analyzed to determine the effect that non-symmetry currents have on the final solution of the network when compared to the balanced scenario.

Notably, the proposed optimization method focusses on planning radial three-phase distribution networks with a pure-radial structure, where the telescopic configuration is naturally provided by the algorithm as a function of the current requirements at each branch. In addition, for the formulation of the three-phase backward/forward power flow, in the case of the loads connected in Y, it is assumed that these are solidly grounded, i.e., no neutral conductor is considered to minimize the planning costs.

The remainder of this document is arranged as follows: Section 2 presents the general formulation of the problem of the optimal selection of calibers in three-phase distribution networks, where the MINLP nature of the network and the effect of the calibers' sizes regarding the investment and operation costs during the planning period are highlighted. Section 3 presents the proposed methodology based on the hybridization of the discrete version of the vortex search algorithm and the three-phase backward/forward power flow in a master-slave connection. Section 4 presents information of all the test feeders as well as the simulation cases, i.e., distribution networks composed of 8 and 27 nodes with balanced and unbalanced load connections. Section 5 presents all the numerical results of the proposed DVSA applied on both test feeders. Section 6 presents numerical comparisons with classical optimization methods reported in the literature, such as tabu search, exact model, and classic and improved versions of the genetic algorithm, along with numerical results considering balanced and unbalanced load cases are studied including Δ- and

Y-connections. Finally, Section 7 presents the main conclusions derived from this research as well as scope for possible future work.

2. Mathematical Formulation

The problem of the optimal selection of the calibers of conductors in electrical distribution grids with balanced (single-phase representation) and unbalanced (three-phase formulation) structures can be formulated mathematically through a MINLP) model [6], in which the binary (or integer) variables are related with the selection of a conductor type for each distribution line, whereas continuous variables are associated with electrical variables such as voltages, currents, and powers [7]. The main complication associated with the MINLP model in determining the optimal set of calibers corresponds to the power balance equations which are indeed nonlinear and non-convex due to the products of the voltages and trigonometric functions [30]. The complete optimization model for the problem studied in this research is presented below.

2.1. Objective Function

The objective function of the problem of the optimal selection of conductors in three-phase balanced and unbalanced distribution networks considering a planning horizon of one year corresponds to the minimization of the investment costs in the calibers of the conductors as well as the costs of the annual energy losses. The general structure of the objective function is presented in Equations (1)–(3), as follows:

$$C_{\text{loss}} = C_p \sum_{h\in\Omega_h}\sum_{p\in\Omega_p}\sum_{q\in\Omega_p}\sum_{i\in\Omega_b}\sum_{j\in\Omega_b} V_{h,i}^{p} V_{h,j}^{q} Y_{ij}^{pq}\left(\lambda_{ij}^{c}\right)\cos\left(\phi_{h,i}^{p}-\phi_{h,j}^{q}-\phi_{h,ij}^{pq}\left(\lambda_{ij}^{c}\right)\right)\Delta_h \quad (1)$$

$$C_{\text{inv}} = \sum_{c\in\Omega_c}\sum_{km\in\Omega_L} C_{km}^{c} L_{km} \lambda_{km}^{c} \quad (2)$$

$$z = \min\left(C_{\text{loss}} + C_{\text{inv}} + C_{\text{pen}}\right) \quad (3)$$

Equation (1) evaluates the costs of the energy losses in the system for the period of study (C_{loss}), where C_p is the average energy costs; T is the number of hours in an ordinary year, i.e., 8760 h; Y_{ij}^{pq} and ϕ_{ij}^{pq} represent the admittance magnitude and angle that relate nodes i and j and phases p and q, respectively, which is a nonlinear function of the type of conductors selected for the distribution grid, i.e., this is a nonlinear function of the binary variable λ_{ij}^{c}; $V_{h,i}^{p}$ and $V_{h,j}^{p}$ represent the voltage magnitudes in nodes i and m for phase p in the period of time h; and $\phi_{h,i}^{p}$ and $\phi_{h,j}^{p}$ are the voltage angles in nodes i and m for the phases p in the period of time h.

Equation (2) calculates the investment costs in calibers of the conductors installed in the three-phase network (C_{inv}), where C_{km} defines the costs of the conductor installed in the route km with caliber type c; L_{km} is the length of the route that connects nodes k and m; and λ_{km}^{c} is the binary variable that defines if the caliber type c is assigned to route km.

Equation (3) corresponds to the sum of the annual energy loss costs with the total investment in conductors, which is also added with the penalization costs associated with the violation of the distribution system constraints, i.e., violation of the thermal bound in conductors. The costs of the penalizations are assigned to the variable C_{pen}.

2.2. Set of Constraints

The set of constraints associated with the problem of the optimal selection of conductors in three-phase distribution networks includes the active and reactive power balance equations, voltage regulation bounds, conductor capabilities, and binary nature of the decision variables. The complete list of constraints is presented below.

$$P_{g_{i,h}}^{p} - P_{d_{i,h}}^{p} = \sum_{p\in\Omega_h}\sum_{q\in\Omega_p}\sum_{i\in\Omega_b}\sum_{j\in\Omega_b} V_{h,i}^{p} V_{h,j}^{q} Y_{ij}^{pq}(\lambda_{ij}^{c})\cos\left(\phi_{h,i}^{p}-\phi_{h,j}^{q}-\phi_{h,ij}^{pq}\left(\lambda_{ij}^{c}\right)\right) \quad \begin{bmatrix}\forall i\in\Omega_b\\ \forall h\in\Omega_h\\ \forall p\in\Omega_p\end{bmatrix} \quad (4)$$

$$Q^p_{g_{i,h}} - Q^p_{d_{i,h}} = \sum_{p\in\Omega_h}\sum_{q\in\Omega_p}\sum_{i\in\Omega_b}\sum_{j\in\Omega_b} V^p_{h,i}V^q_{h,j}Y^{pq}_{ij}(\lambda^c_{ij})\sin\left(\phi^p_{h,i} - \phi^q_{h,j} - \phi^{pq}_{h,ij}\left(\lambda^c_{ij}\right)\right) \quad \begin{bmatrix}\forall i \in \Omega_b\\ \forall h \in \Omega_h\\ \forall p \in \Omega_p\end{bmatrix} \tag{5}$$

$$I^p_{km,h} = f\left(V^p_{h,k}, V^p_{h,m}, \phi^p_{h,k}, \phi^p_{h,m}, \lambda^c_{km}, R^c_{km}, X^c_{km}\right), \quad \begin{bmatrix}\forall\{km\} \in \Omega_L\\ \forall h \in \Omega_h\\ \forall p \in \Omega_p\end{bmatrix} \tag{6}$$

$$\left|I^p_{km,h}\right| \leq \sum_{c\in\Omega}\lambda^c_{km}I^{\max}_c, \quad \begin{bmatrix}\forall\{km\} \in \Omega_L\\ \forall h \in \Omega_h\\ \forall p \in \Omega_p\end{bmatrix} \tag{7}$$

$$V^{\min}_i \leq V^p_{i,h} \leq V^{\max}_i, \quad \begin{bmatrix}\forall i \in \Omega_b\\ \forall h \in \Omega_h\\ \forall p \in \Omega_p\end{bmatrix} \tag{8}$$

$$\sum_{c\in\Omega_c}\lambda^c_{km} = 1 \ \ [\forall\{km\} \in \Omega_L] \tag{9}$$

$$\sum_{km\in\Omega_L}\sum_{c\in\Omega_c}\lambda^c_{km} = n - 1 \tag{10}$$

$$\lambda^c_{km} \in \{0,1\} \ \ [\forall\{km\} \in \Omega_L, \forall c \in \Omega_c] \tag{11}$$

For equations ranging from (4) to (11), the set Ω_L contains the lines of the distribution system, the set Ω_h contains all the load duration periods, the set Ω_b contains all nodes of the distribution system, and the set Ω_p contains the phases of the system.

Equations (4) and (5) define the active and reactive power balance for each node, for each phase, and for each time period, where $P^p_{g_{i,h}}$ and $Q^p_{g_{i,h}}$ are the active and reactive power generations, and $P^p_{d_{i,h}}$ and $Q^p_{d_{i,h}}$ the active and reactive power demands, respectively. Equation (6) defines the nonlinear function that calculates the current flow ($I^p_{km,h}$) in the route km in the time period h for the phase p, which is a function of the voltage magnitudes and angles as well as the conductor size and their parameters, i.e., resistances (R^c_{km}) and reactances (X^c_{km}).

Inequality constraint (7) allows guaranteeing that the current flow in route km in the time period h for the phase p must be lower than or equal to the thermal bound of the caliber selected for this route, i.e., $I^{\max}_c$. The box-type constraint (8) ensures the voltage regulation bounds for all the voltages per node, phase, and period of time, with $V^{\min}_i$ and $V^{\max}_i$ being the lower and upper voltage limits, respectively. Equation (9) guarantees that for the route between nodes k and k, only one type of caliber c is selected for the conductor, and (10) ensures that the amount of the conductors selected for the distribution system is equal to the $n-1$ nodes, i.e., radiality structure of the grid [6]. Finally, Equation (11) defines the binary nature of the decision variables regarding the selection of the caliber type c for each route km.

Remark 1. *The MINLP model defined from (1) to (11) corresponds to a general formulation for the problem of the optimal selection of conductors in three-phase distribution networks with balanced and unbalanced structures. The main complications of this model are as follows: (i) existence of binary variables; (ii) strong nonlinearities in the power balance and objective functions; and (iii) the necessity for recalculating the admittance nodal matrix for each combination of the conductors. To deal with these difficulties in the mathematical model of the studied problem, we propose a master-slave optimization approach to solve the MINLP model based on the vortex search algorithm and a three-phase power flow method.*

3. Proposed Methodology

To solve the problem of the optimal selection of calibers in distribution networks with balanced and unbalanced loads to minimize the investment and operation costs, in this research, the application of a master-slave optimization approach is proposed. The master

stage is the discrete version of the vortex search algorithm that deals with the optimal selection of calibers for all routes using an integer codification [28]. In the slave stage, each configuration of the conductors is evaluated with a three-phase backward/forward power-flow method that determines the total costs of energy losses for the planning period [5]. In the following subsections, the main aspects of the master and slave stages are presented.

3.1. Master Stage: DVSA

The vortex search algorithm is a relatively newly developed metaheuristic optimization algorithm that deals with continuous and integer optimization problems [31]. The main advantages of this algorithm are the possibility of exploring and exploiting the solution space with hyper-ellipses with variable radius [32]. The exploration and exploitation of the solution space are performed by generating candidate solutions around the center of the hyper-ellipse (best current solution) with a Gaussian distribution probability that allows sweeping the solution space uniformly [29]. In this research, due to the integer nature of the studied problem, we employed a discrete version of the vortex search algorithm proposed in [5] to determine the set of calibers that must be installed in all distribution lines. For this purpose, an integer codification was employed to represent a candidate solution of the problem.

3.1.1. Initial Solution

The DVSA works with a variable radius to explore and exploit the solution space. Initially, the hyper-ellipse is at the middle of the solution space, i.e., μ_0 as follows:

$$\mu_0 = \frac{x^{\min} + x^{\max}}{2} \tag{12}$$

where $x^{\min} \in \mathcal{N}^{d\times 1}$ and $x^{\max} \in \mathcal{N}^{d\times 1}$ are integer vectors with dimension d, with d being the dimension of the solution space.

3.1.2. Generation of the Candidate Solutions

The generation of candidate solutions, i.e., $C_i^t(x) = s_i^t = \{x_1, x_2, ..., x_i, ..., x_d\}$ (where i is associated with the ith individual in the current population), is made with a normal Gaussian distribution that has the following structure.

$$S_i^t = p(\zeta_i^t,\ \mu_t, \nu) = \left((2\pi)^d |\nu|\right)^{1/2} e^{\left(-\frac{1}{2}\frac{(\zeta_i^t-\mu_t)^\tau(\zeta_i^t-\mu_t)}{\nu}\right)} \tag{13}$$

where $\zeta_i^t \in \mathbb{R}^{d\times 1}$ is a vector with dimension d filled by random values, $\mu_t \in \mathbb{N}^{d\times 1}$ represents the center of the hyper-ellipse at the iteration t, and $\nu \in \mathbb{R}^{d\times d}$ is the matrix of co-variances. This matrix is simplified as recommended in [5] by a matrix with identical values in its diagonal σ_0 and null values outside its diagonal. The value of σ_0 can be determined as follows:

$$\sigma_0 = \frac{\max\{x^{\max}\} - \min\{x^{\min}\}}{2} \tag{14}$$

where $\nu = \sigma_0 I_{d\times d}$, and $I_{d\times d}$ is an identity matrix with appropriate dimensions. Note that to initialize the radius of the hyper-ellipse, i.e., $(r_t,$ with $t = 0)$, is recommended in the literature as σ_0 [32]. In the DVSA, one of the main variables in the exploration and exploitation of the solution space corresponds to the variable radius because this governs the vector of random variables ζ_i^t as $\zeta_i^t = r_t \text{rand}(d)$, with $\text{rand}(d)$ being a vector with random variables between 0 and 1.

3.2. Bounding the Candidate Solution

When the Gaussian distribution is employed to generate all candidate solutions, there exists the possibility of having a solution outside of the boundaries of the solution space; therefore, for each s_i^t, it is necessary to revise its lower and upper bounds as described below:

$$s_i^t = \begin{cases} s_i^t & x^{\min} \leq x \leq x^{\max} \\ \text{round}\left(x^{\min} + \left(x^{\max} - x^{\min}\right)\text{rand}\right) & \text{otherwise} \end{cases} \tag{15}$$

where rand is a random number between 0 and 1. Notably, that each candidate solution must be an integer. To ensure this integer characteristic of the solution, used the round operator is used.

3.2.1. Choosing the New Center

To advance the exploration and exploitation of the solution space, a new center of the hyper-ellipse must be selected [29]. For doing so, the variable μ_{t+1} must be selected as the best individual contained in $C_i^t(x)$ such that it presents the minimum current objective function value, which implies that μ_{t+1} is selected as $s_{i,best}^t$.

3.2.2. Radius Reduction Process

To make the reduction of the hyper-ellipse radius the initial proposal, [29] recommend the use of an inverse incomplete gamma function; however, for the purpose of simplicity, authors in [32] presented an alternative methodology using an exponential decreasing rule that can be implemented easily in any programming environment. This exponential rule is presented as follows:

$$r_{t+1} = \sigma_0 \left(1 - \frac{t}{t_{\max}}\right) e^{\left(-a\frac{t}{t_{\max}}\right)} \tag{16}$$

where a corresponds to a parameter that governs the speed with the radius of the hyper-ellipse reduced, which is directly associated with the balance of the exploration and exploitation of the solution space. Authors of [32] proposed a heuristic value of 6 for this parameter. In addition, observe that $t_{\max}$ represents the maximum number of iterations of the problem.

3.2.3. General Flow Diagram of the DVSA

The general optimization procedure using the DVSA is summarized in Figure 1, which was adapted from [31].

3.3. Slave Stage: Backward/Forward Three-Phase Power Flow

In general, the three-phase power flow problem in electrical distribution networks is addressed using numerical methods (iterative procedures) due to the nonlinear non-convex structure of the power balance Equations (4) and (5). Therefore, in this section, the general implementation of three-phase backward/forward power flow is illustrated for distribution networks based on its matricial formulation using a small test feeder example, as presented in [5]. To implement the backward/forward power-flow method, consider the electrical distribution network presented in Figure 2. In addition, for this test feeder, we consider the demand information reported in Table 2, and a unique impendance matrix defined in (17) for all lines.

$$Z = \begin{pmatrix} 0.037 + j0.0141 & 0.001 + j0.0068 & 0.001 + j0.0071 \\ 0.001 + j0.0068 & 0.037 + j0.0141 & 0.001 + j0.0067 \\ 0.001 + j0.0071 & 0.001 + j0.0067 & 0.037 + j0.0141 \end{pmatrix} \tag{17}$$

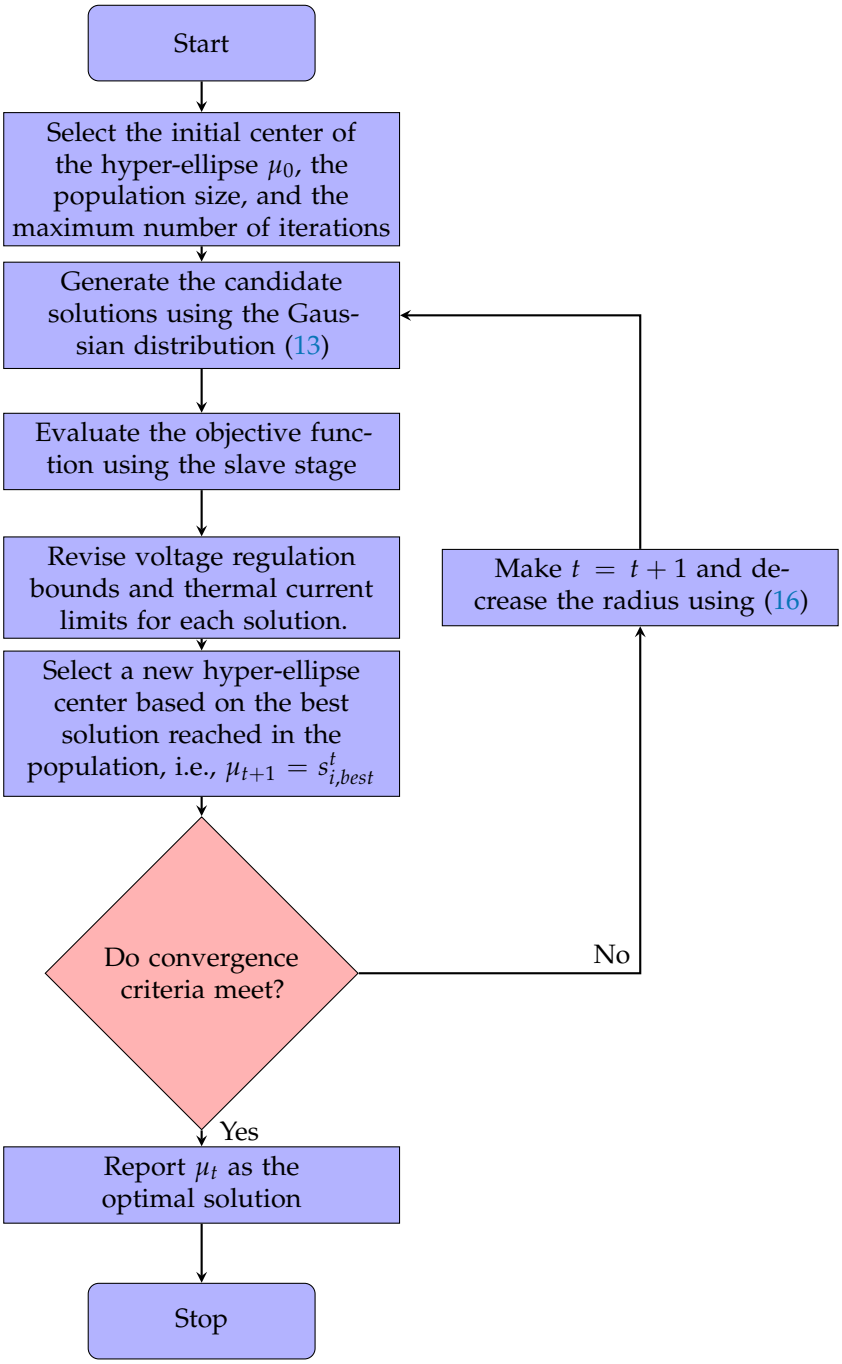

Figure 1. Flow chart for the discrete version of the vortex search algorithm [31].

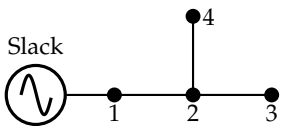

Figure 2. Distribution test feeder composed of four nodes.

Table 2. Active and reactive power consumption.

Node	S_a	S_b	S_c
2	$0.30 + j0.20$	$0.10 + j0.23$	$0.30 + j0.10$
3	$0.26 + j0.02$	$0.02 + j0.10$	$0.30 + j0.02$
4	$0.21 + j0.05$	$0.21 + j0.05$	$0.21 + j0.05$

The main characteristic of the three-phase backward/forward power flow is the usage of admittance matrices to obtain a general formulation that can work with radial and meshed distribution grids. The first step in the power-flow formulation corresponds to the formation of an incidence matrix, which takes the following form in the single- and three-phase forms:

$$A_{1\phi} = \begin{bmatrix} 1 & 0 & 0 \\ -1 & 1 & 1 \\ 0 & -1 & 0 \\ 0 & 0 & -1 \end{bmatrix} \quad \Longrightarrow \quad A_{3\phi} = \begin{bmatrix} 1 & 0 & 0 & 0 & 0 & 0 & 0 & 0 & 0 \\ 0 & 1 & 0 & 0 & 0 & 0 & 0 & 0 & 0 \\ 0 & 0 & 1 & 0 & 0 & 0 & 0 & 0 & 0 \\ -1 & 0 & 0 & 1 & 0 & 0 & 1 & 0 & 0 \\ 0 & -1 & 0 & 0 & 1 & 0 & 0 & 1 & 0 \\ 0 & 0 & -1 & 0 & 0 & 1 & 0 & 0 & 1 \\ 0 & 0 & 0 & -1 & 0 & 0 & 0 & 0 & 0 \\ 0 & 0 & 0 & 0 & -1 & 0 & 0 & 0 & 0 \\ 0 & 0 & 0 & 0 & 0 & -1 & 0 & 0 & 0 \\ 0 & 0 & 0 & 0 & 0 & 0 & -1 & 0 & 0 \\ 0 & 0 & 0 & 0 & 0 & 0 & 0 & -1 & 0 \\ 0 & 0 & 0 & 0 & 0 & 0 & 0 & 0 & -1 \end{bmatrix} \tag{18}$$

Note that in (18), the incidence matrix in the single-phase equivalent, i.e., $A_{1\phi}$, has n rows and b columns, with n being the number of nodes and b the number of branches, which implies that this matrix is known as the node-to-branch incidence matrix. In addition, in the three-phase case, the dimensions increase to $3n \times 3b$. Now, the three-phase node-to-branch incidence matrix can be divided in two components, which are associated with the generation and demand nodes, as follows:

$$A_{3\phi} = \begin{bmatrix} A_{g3\phi} \\ A_{d3\phi} \end{bmatrix} \tag{19}$$

Now, the three-phase impedance matrix that contains information of each line three-phase impedance matrices is constructed, which produces the following structure for the test feeder presented in Figure 2.

$$Z_{3\phi} = \begin{bmatrix} Z_{11} & Z_{12} & Z_{13} & 0 & 0 & 0 & 0 & 0 & 0 \\ Z_{21} & Z_{22} & Z_{23} & 0 & 0 & 0 & 0 & 0 & 0 \\ Z_{31} & Z_{32} & Z_{33} & 0 & 0 & 0 & 0 & 0 & 0 \\ 0 & 0 & 0 & Z_{11} & Z_{12} & Z_{13} & 0 & 0 & 0 \\ 0 & 0 & 0 & Z_{21} & Z_{22} & Z_{23} & 0 & 0 & 0 \\ 0 & 0 & 0 & Z_{31} & Z_{32} & Z_{33} & 0 & 0 & 0 \\ 0 & 0 & 0 & 0 & 0 & 0 & Z_{11} & Z_{12} & Z_{13} \\ 0 & 0 & 0 & 0 & 0 & 0 & Z_{21} & Z_{22} & Z_{23} \\ 0 & 0 & 0 & 0 & 0 & 0 & Z_{31} & Z_{32} & Z_{33} \end{bmatrix} \tag{20}$$

Because the general formulation of the matricial backward/forward three-phase power-flow method works with admittance nodal matrices that associate generation and

demand nodes among them [5], when the components of the node-to-branch incidence and the impedance matrix is considered, we obtain the following admittance components:

$$Y_{g3\phi} = A_{d3\phi} {Z_{3\phi}}^{-1} {A_{g3\phi}}^{T} \tag{21}$$

$$Y_{d3\phi} = A_{d3\phi} {Z_{3\phi}}^{-1} {A_{d3\phi}}^{T} \tag{22}$$

Note that with the general admittance matrices defined in (21) and (22), the following recursive power-flow formula for backward/forward three-phase power flow is formulated [33].

$${V_{d3\phi}}^{m+1} = -{Y_{d3\phi}}^{-1} \left({I_{d3\phi}}^{m} + Y_{g3\phi} V_{g3\phi} \right). \tag{23}$$

where m is the iterative counter.

The recursive three-phase power-flow formula defined in (23) is evaluated from the initial value (i.e., starting point) until the convergence criterion is met, which is defined below:

$$|{V_{d3\phi}}^{m+1} - {V_{d3\phi}}^{m}| < \varepsilon \tag{24}$$

where ε is the error of convergence, which is typically set to 1×10^{-10}.

Note that the recursive formula (23) depends on the current calculated at the demand nodes, i.e., ${I_{d3\phi}}^{m}$, which can be calculated using two methods as a function of the type of load connection (Y and Δ). To show the method of calculating the load current for loads with Y- and Δ- connections, consider the following formulas applied to node k:

$$I_{k3\phi} = \begin{pmatrix} I_{ka} \\ I_{kb} \\ I_{kc} \end{pmatrix} = \begin{pmatrix} \left(\frac{S_{ka}}{V_{ka}} \right)^{*} \\ \left(\frac{S_{kb}}{V_{kb}} \right)^{*} \\ \left(\frac{S_{kc}}{V_{kc}} \right)^{*} \end{pmatrix}, \ \forall k \in \Omega_b \ \{Y - \text{connection}\} \tag{25}$$

$$I_{k3\phi} = \begin{pmatrix} I_{ka} \\ I_{kb} \\ I_{kc} \end{pmatrix} = \begin{pmatrix} \left(\frac{S_{ka}}{V_{ka} - V_{kb}} \right)^{*} - \left(\frac{S_{kc}}{V_{kc} - V_{ka}} \right)^{*} \\ \left(\frac{S_{kb}}{V_{kb} - V_{kc}} \right)^{*} - \left(\frac{S_{ka}}{V_{ka} - V_{kb}} \right)^{*} \\ \left(\frac{S_{kc}}{V_{kc} - V_{ka}} \right)^{*} - \left(\frac{S_{kb}}{V_{kb} - V_{kc}} \right)^{*} \end{pmatrix}, \ \forall k \in \Omega_b \ \{\Delta - \text{connection}\} \tag{26}$$

Typically, for power-flow analysis, the per-unit representation of all electrical variables is used, which implies that the substation voltage can be defined using a positive sequence as follows: $V_{g3\phi} = [1\angle 0^{\circ},\ 1\angle -120^{\circ},\ 1\angle 120^{\circ}]^{T}$; in addition, all demand voltages initially defined in $m = 0$ are defined as $V_{k3\phi} = V_{g3\phi}$.

To summarize the general procedure of the backward/forward three-phase power flow for loads with Y- and Δ-connections, consider the flow diagram presented in Figure 3.

Finally, with all voltages provided by the solution of the recursive Formula (23), using the iterative procedure in Figure 3, the amount of power losses of the network is calculated, i.e., P_{loss}, as follows:

$$P_{\text{loss}} = \left(V_{3\phi}^{m+1} \right)^{T} \left(I_{3\phi}^{m+1} \right)^{\star}, \tag{27}$$

where $V_{3\phi}^{m+1}$ and $I_{3\phi}^{m+1}$ are vectors with all voltages and net injected currents of the network including the slack source.

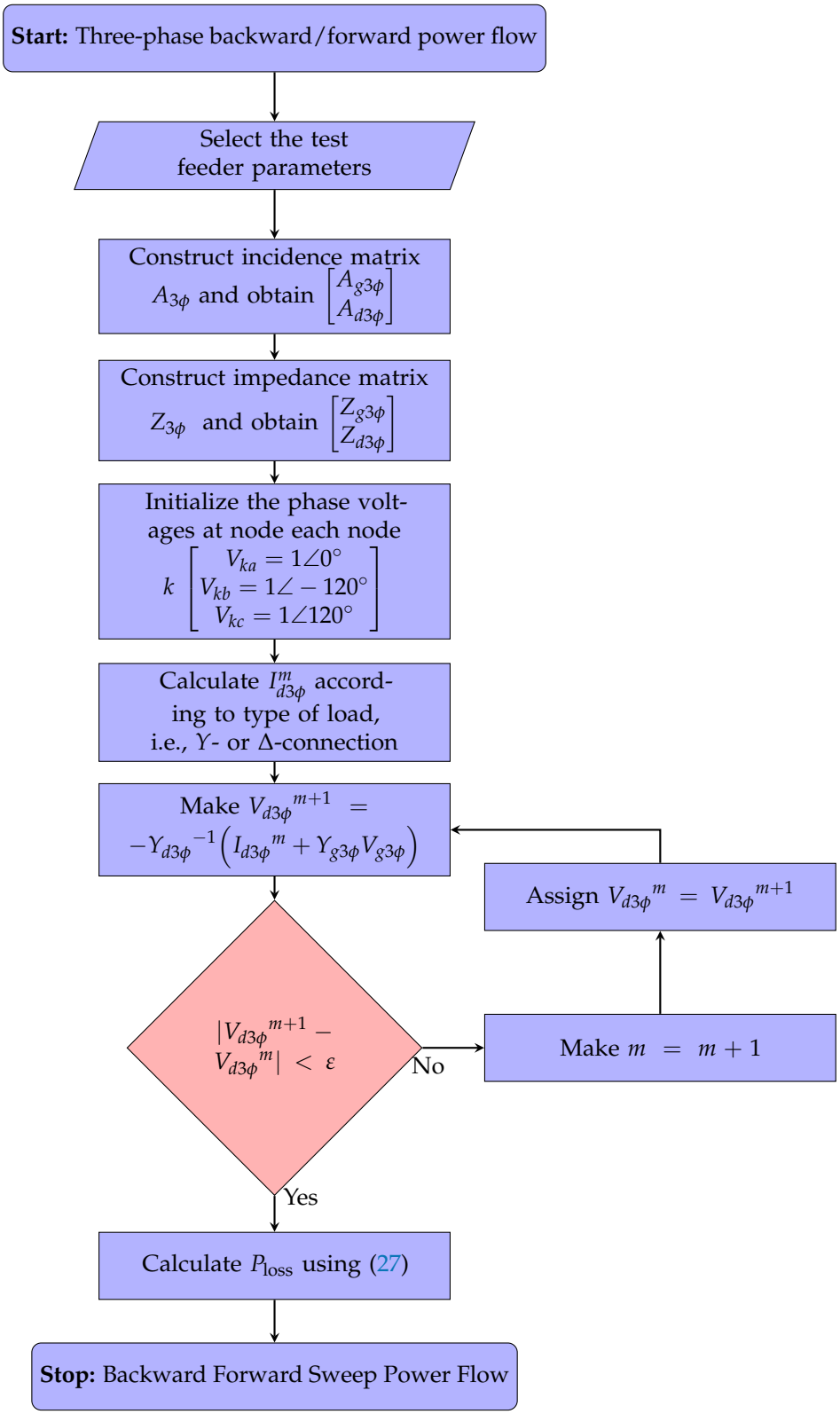

Figure 3. Flowchart for three-phase backward/forward power flow.

The solution of the three-phase power flow problem using the backward/forward approach for the numerical example is reported in Table 3, which also compared the results with those obtained using the Newton-Raphson method available in the DigSILENT software.

Table 3. Voltages in the small test example with pure *Y*-connected loads (all values in pu).

	DigSILENT		MATLAB		Errors	
Voltage	**Magnitude**	**Angle**	**Magnitude**	**Angle**	**Voltage Error (%)**	**Angle Error (%)**
V_{2a}	0.9725	0.21	0.9725	0.21	0.000	0.000
V_{2b}	0.9840	−119.18	0.9840	−119.18	0.000	0.000
V_{2c}	0.9660	119.89	0.9660	119.90	0.000	0.008
V_{3a}	0.9647	0.11	0.9647	0.10	0.000	0.000
V_{3b}	0.9821	−118.86	0.9821	−118.86	0.000	0.000
V_{3c}	0.9531	119.72	0.9530	119.72	0.010	0.000
V_{4a}	0.9644	0.22	0.9643	0.22	0.010	0.000
V_{4b}	0.9759	−119.16	0.9760	−119.17	0.010	0.008
V_{4c}	0.9577	119.91	0.9576	119.92	0.010	0.008

Notably, the bases used for this example were 13.8 kV and 1000 kVA; thus, the power loss results shown in Table 4 are already in real values.

Table 4. Performance of the power-flow methods.

Method	**Iterations**	**Active Power Losses (kW)**
DigSILENT	3	74.1634
MATLAB	8	74.1645

From the numerical results in Table 4, we can observe that the backward/forward power-flow method programmed in the MATLAB environment takes 8 iterations, whereas the classical Newton-Raphson takes 3 iterations; however, this difference is due to two aspects: first, the tolerance error assigned in the DigSILENT software which is 1×10^{-6} at maximum, whereas the backward/forward is set with a tolerance of 1×10^{-10}; and second, the backward/forward does not use derivatives in its formulation, which naturally increases the number of iterations when compared with the Newton-Raphson method which works with the Jacobian matrix.

Notably, the main advantage of using the backward/forward in the MATLAB environment is the possibility of evaluating thousands of three-phase power flows to solve the problem of the optimal selection of the calibers of the conductors with a simple master-slave optimization approach, as described in the previous sections with low processing times, as demonstrated in [5].

4. Test Feeders and Simulation Scenarios

In this section, the main characteristics of the two radial distribution feeders composed of 8 and 27 nodes, respectively, are presented. In addition, two study cases will be analyzed. The first case corresponds to the analysis of the test feeders operated under balanced load connections, while the second case works with high load unbalances. Notably, for each study case, we will consider three load behavior scenarios for a planning horizon of one year.

The general parameters of the proposed master-slave optimization approach are listed in Table 5.

Table 5. General simulation parameters.

Parameter	**Value**	**Unit**
Energy cost	0.1390	(US$/year)
Iterations	1000	—
Neighborhood size	20	—
Tolerance	1×10^{-10}	—

4.1. First Simulation Case

In this simulation case, it is considered that the test feeders composed of 8 and 27 nodes work with loads perfectly balanced. In addition, the information reported in Tables 6 and 7 correspond to the load per phase, and the nominal voltage is defined phase-to-ground.

4.1.1. Test Feeder 1 (Balanced)

The first test feeder is a three-phase distribution grid reported in [10,23,34] to study the problem of the optimal selection of the calibers of conductors in distribution grids. This test feeder works with a nominal voltage of 13.8 kV, where the substation node corresponds to bus 1; in addition, all loads operate with unity power factor. The single-line diagram of this test feeder is presented in Figure 4.

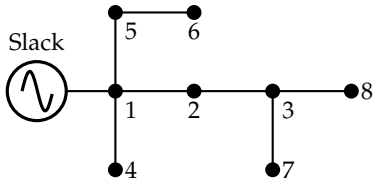

Figure 4. Single-line diagram of the 8-bus test feeder.

Table 6 presents information regarding branches (number and length) and information regarding constant power consumptions.

Table 6. Parametric information of the 8-bus test feeder for the balanced case.

Branch	Bus i	Bus j	L_{ij} (km)	$P^D_{j,h}$ (kW)	$Q^D_{j,h}$ (kvar)
1	1	2	1.00	1054.2	0
2	2	3	1.00	806.5	0
3	1	4	1.00	2632.5	0
4	1	5	1.00	609.0	0
5	5	6	1.00	2034.5	0
6	3	7	1.00	932.8	0
7	3	8	1.00	1731.4	0

4.1.2. Second Test Feeder (Balanced)

This test feeder corresponds to a three-phase network comprising 27 nodes (1 slack and 26 demands), which work with 13.8 kV at the substation node. This test system was reported in [10] to analyze the problem of the optimal conductor size selection using the tabu search algorithm. The single-phase diagram of this 27-bus system is depicted in Figure 5.

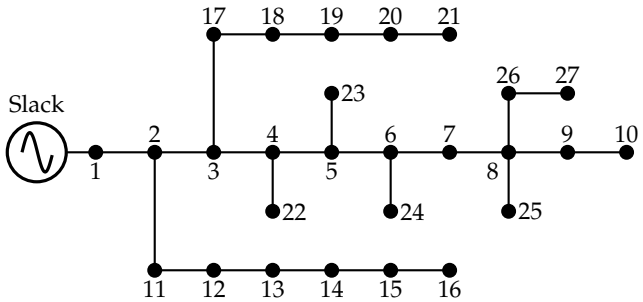

Figure 5. Single-line diagram of the 27-bus test feeder.

Table 7 presents information regarding branches (number and length) and information regarding constant power consumptions.

Table 7. Parametric information of the 27-bus test feeder for the balanced case.

Branch	Bus i	Bus j	L_{ij} (km)	$P_{j,h}^{D}$ (kW)	$Q_{j,h}^{D}$ (kvar)
1	1	2	0.55	0	0
2	2	3	1.50	0	0
3	3	4	0.45	297.5	184.4
4	4	5	0.63	0	0
5	5	6	0.70	255	158
6	6	7	0.55	0	0
7	7	8	1.00	212.5	131.7
8	8	9	1.25	0	0
9	9	10	1.00	266.1	164.9
10	2	11	1.00	85	52.7
11	11	12	1.23	340	210.7
12	12	13	0.75	297.5	184.4
13	13	14	0.56	191.3	118.5
14	14	15	1.00	106.3	65.8
15	15	16	1.00	255	158
16	3	17	1.00	255	158
17	17	18	0.60	127.5	79
18	18	19	0.90	297.5	184.4
19	19	20	0.95	340	210.7
20	20	21	1.00	85	52.7
21	4	22	1.00	106.3	65.8
22	5	23	1.00	55.3	34.2
23	6	24	0.40	69.7	43.2
24	8	25	0.60	255	158
25	8	26	0.60	63.8	39.5
26	26	27	0.80	170	105.4

4.2. Second Simulation Case

In this simulation case, the single-phase diagram for the 8- and 27-bus systems depicted in Figures 4 and 5 is also considered; however, the main characteristic is that both the test feeders have highly unbalanced loads. The unbalanced information of the loads for both test feeders is reported in Tables 8 and 9.

Table 8. Parametric information of the 8-bus test feeder for the unbalanced case.

Branch	Bus i	Bus j	L_{ij} (km)	$P_{j,a}^{D}$ (kW)	$Q_{j,a}^{D}$ (kvar)	$P_{j,b}^{D}$ (kW)	$Q_{j,b}^{D}$ (kvar)	$P_{j,c}^{D}$ (kW)	$Q_{j,c}^{D}$ (kvar)
1	1	2	1.00	3162.6	0	0	0	0	0
2	2	3	1.00	0	0	2419.5	0	0	0
3	3	4	1.00	0	0	0	0	7897.5	0
4	2	5	1.00	913.5	0	913.5	0	0	0
5	5	6	1.00	0	0	3051.6	0	3051.6	0
6	2	7	1.00	2798.4	0	0	0	0	0
7	3	8	1.00	1298.55	0	2597.1	0	1298.55	0

4.3. Simulation Scenarios

To have a wide panorama regarding different operating practices of the distribution companies, here, we present three possible demand scenarios for planning the distribution grid. The first scenario, i.e., $S1$, refers to a distribution network operated during all the planning periods with 100% of its load consumption, that is, the planning project is considered the peak load case. The second scenario, i.e., $S2$, considers a duration load curve composed of three periods to distribute all hours in an ordinary year (8760 h) as follows: 100% of the demand during 1000 h, 60% of the peak demand during 6760 h, and

30% peak load consumption during the remaining 1000 h. Finally, the third scenario, i.e., *S*3, considers a typical daily load curve with the profile reported in [35]. The load profile curve and its values are reported in Figure 6 and Table 10, respectively.

Table 9. Parametric information of the 27-bus test feeder for the unbalanced case.

Branch	Bus i	Bus j	L_{ij} (km)	$P^D_{j,a}$ (kW)	$Q^D_{j,a}$ (kvar)	$P^D_{j,b}$ (kW)	$Q^D_{j,b}$ (kvar)	$P^D_{j,c}$ (kW)	$Q^D_{j,c}$ (kvar)
1	1	2	0.55	0	0	0	0	0	0
2	2	3	1.5	0	0	0	0	0	0
3	3	4	0.45	892.5	553.2	0	0	0	0
4	4	5	0.63	0	0	0	0	0	0
5	5	6	0.7	0	0	765	474	0	0
6	6	7	0.55	0	0	0	0	0	0
7	7	8	1	0	0	0	0	637.5	395.1
8	8	9	1.25	0	0	0	0	0	0
9	9	10	1	0	0	0	0	798.3	494.7
10	2	11	1	0	0	255	158.1	0	0
11	11	12	1.23	1020	632.1	0	0	0	0
12	12	13	0.75	446.25	276.6	446.25	276.6	0	0
13	13	14	0.56	0	0	286.95	177.75	286.95	177.75
14	14	15	1	159.45	98.7	0	0	159.45	98.7
15	15	16	1	0	0	382.5	237	382.5	237
16	3	17	1	1	0	765	474	0	0
17	17	18	0.6	382.5	237	0	0	0	0
18	18	19	0.9	446.25	276.6	446.25	276.6	0	0
19	19	20	0.95	0	0	510	316.05	510	316.05
20	20	21	1	127.5	79.05	0	0	127.5	79.05
21	4	22	1	0	0	159.75	98.7	159.75	98.7
22	5	23	1	165.9	102.6	0	0	0	0
23	6	24	0.4	0	0	0	0	209.1	129.6
24	8	25	0.6	255	158	255	158	255	158
25	8	26	0.6	63.8	39.5	63.8	39.5	63.8	39.5
26	26	27	0.8	170	105.4	170	105.4	170	105.4

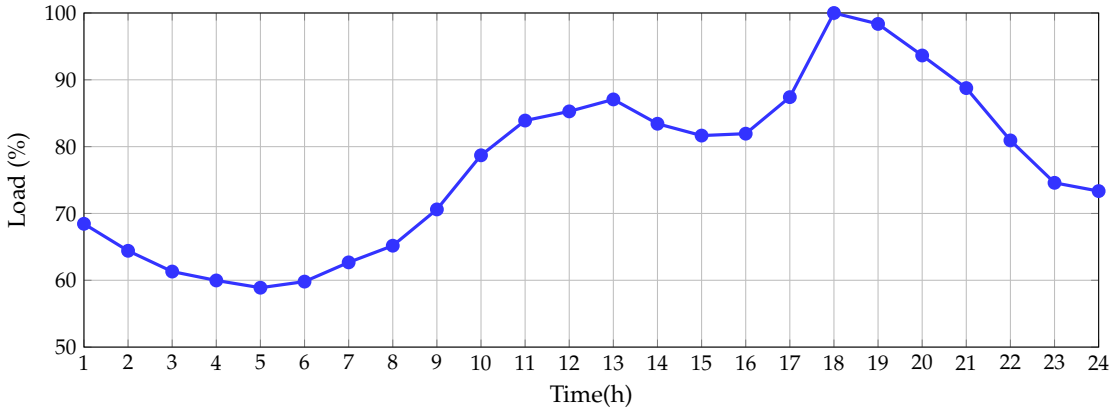

Figure 6. Typical demand load curve.

Table 10. Data for the typical load curve in the *S*3.

Time (h)	Power (pu)	Time (h)	Power (pu)
1	0.684511335	13	0.870642027
2	0.64412269	14	0.834254144
3	0.613069156	15	0.816536483
4	0.599733283	16	0.81939417
5	0.588874071	17	0.874071252
6	0.59801867	18	1
7	0.626786054	19	0.983615927
8	0.651743189	20	0.936368832
9	0.706039246	21	0.887597638
10	0.787007049	22	0.809297009
11	0.839016956	23	0.745856354
12	0.852733854	24	0.733473042

4.4. Set of Conductors Available

To determine the optimal set of calibers assigned to each of the studied test feeders in all simulation cases, we consider 8 different types of conductors. This set is reported in Table 11, where their impedances, maximum thermal currents, and cost per kilometer are presented. Notably, this information has been adapted from [23].

Table 11. Set of conductors considered in all the numerical validations.

Caliber (c)	r (Ω/km)	x (Ω/km)	$I^{c,\max}$ (A)	C^c (US$/km)
1	0.8763	0.4133	180	1986
2	0.6960	0.4133	200	2790
3	0.5518	0.4077	230	3815
4	0.4387	0.3983	270	5090
5	0.3480	0.3899	300	8067
6	0.2765	0.3610	340	12,673
7	0.0966	0.1201	600	23,419
8	0.0853	0.0950	720	30,070

5. Computational Validation

Numerical validation of the proposed master-slave optimization approach was performed in the MATLAB programming environment with the 2021*b* version in a personal computer with processor Intel(R) Core(TM) i5-2410M CPU @ 2.30 GHz, 2301 Mhz, 6 Gb RAM and the Microsoft Windows 10 Home x64 operative system. It is worth mentioning that all simulations were performed considering the parameters reported in Table 4 for the algorithm parametrization.

In this section, we present the results for both test feeders considering the proposed master-slave optimization approach with balanced and unbalanced cases, including all three load profiles.

5.1. Results for Simulation Case 1

Here, we present all numerical results for the 8- and 27-bus systems presented in Figures 4 and 5 considering all simulation scenarios and balanced and unbalanced load cases.

5.1.1. Numerical Results in the 8-Bus Test System

After applying the proposed DVSA combined with the backward/forward power flow method to select the set of optimal calibers in the 8-bus system for all the load scenarios, the results in Table 12 are attained.

Table 12. Investment and operating costs in the 8-bus test system for the balanced load case.

Scenario	Investment in Conductors (US$)	Technical Losses (US$)	Objective Function (US$)
S1	163,350	345,007.959	508,357.959
S2	112,677	171,321.866	283,998.867
S3	129,258	236,968.262	366,226.262

The results in Table 12 show that (i) *S*1 presents the higher annual costs because the annual costs of the energy losses are higher when compared with the remaining simulation cases because for all the periods of time, the load consumption is maximum, which also is directly associated with the increment in the investment costs of the calibers; (ii) *S*2 is the most optimistic planning case because it reduces the planning costs by approximately 44.13% with respect to *S*1; this is attributable to the fact that during 6760 hours of the year, the load is the 60% of the peak case, which clearly reduces the costs of the power losses by approximately 50.34% with respect to the full load case. This reduction in the cost of the annual energy losses has a direct effect on the set of calibers selected by reducing it by approximately US$50673 with respect to *S*1; (iii) *S*3 can be considered the more realistic simulation case because this captures the daily variations on the load profile, which have a direct effect on the annual energy losses and the total investment in the calibers; notably, this scenario is the intermediate simulation case with respect to the total planning case when compared with *S*1 and *S*3.

In contrast, Table 13 presents a set of calibers selected for the 8-bus test feeder with the balanced case for all the simulation scenarios. Note that *S*1 has calibers with higher dimensions when compared with the other two scenarios, whereas *S*2 has calibers with the minimum dimensions, and *S*3 has an intermediate solution in terms of the calibers, which is completely coincident with the costs of the conductors reported in Table 12. However, it is important to mention that for all the scenarios, line 1 has the same caliber, which is because in all cases, there exists a period of time where the load is maximum, which implies that the thermal bound must always be respected, which is only possible with caliber type 6.

Table 13. Calibers selected for the 8-bus system in the balanced load case.

Branch	Scenario 1	Scenario 2	Scenario 3
1	6	6	6
2	6	4	5
3	5	4	4
4	5	4	4
5	4	3	4
6	2	1	1
7	4	3	4

In contrast, Figure 7 shows the voltage profiles in the eight nodes of the balanced system, where it can be seen that the voltage value is never lower than 0.979 pu, and this is the value of the voltage of node 8 in *S*2.

5.1.2. Numerical Results in the 27-Bus Test System

After applying the proposed DVSA combined with the backward/forward power-flow method, to select the set of optimal calibers in the 27-bus system for all load scenarios, the results in Table 14 are attained.

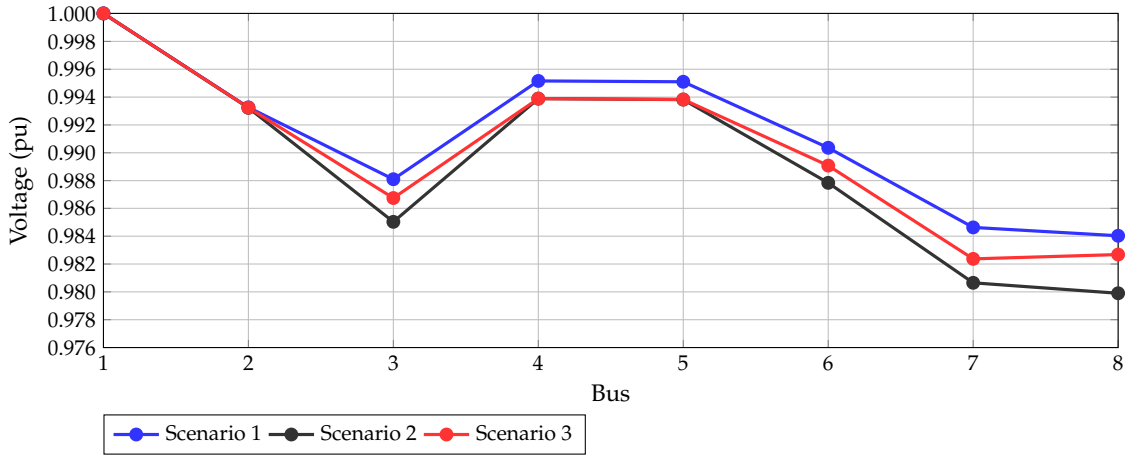

Figure 7. Voltage profile at each node for the hour of maximum demand in the three stages of case 1 of test system 1.

Table 14. Investment and operating costs in test system 2.

Scenario	Investment in Conductors (US$)	Technical Losses (US$)	Objective Function (US$)
S1	344,352.15	217,672.327	562,024.478
S2	232,566.51	155,671.759	388,238.269
S3	279,480.00	196,153.637	475,633.637

From the results in Table 14, we note that (i) *S*1 presents higher annual costs because the annual costs of the energy losses are higher when compared with the remaining simulation cases because for all the periods of time, the load consumption is maximum, which is also directly associated with the increment in the investment costs of the calibers; (ii) *S*2 is the most optimistic planning case because it reduces the planning costs by approximately 69.08% with respect to *S*1; this is attributable to the fact that during 6760 h of the year, the load is 60% that of the peak case, which clearly reduces the costs of the power losses by approximately 71.52% with respect to the full load case. This reduction in the cost of the annual energy losses has a direct effect on the set of calibers selected, and the losses are reduced by approximately US$111,785.64 with respect to *S*1; (iii) *S*3 can be considered the more realistic simulation case because this captures the daily variations on the load profile, which has a direct effect on the annual energy loss costs and the total investment in the calibers; notably, this scenario is an intermediate simulation case with respect to the total planning case when compared with *S*1 and *S*3.

In contrast, Table 15 presents a set of calibers selected for the 27-bus test feeder with the balanced case for all the simulation scenarios. Note that *S*1 has calibers with higher dimensions when compared with the other two scenarios, whereas *S*2 has calibers with minimum dimensions, and *S*3 has an intermediate solution in terms of the calibers, which is completely coincident with the costs of the conductors reported in Table 14. However, it is important to mention that for all the scenarios, line 1 has the same caliber, which is due to the fact that in all the cases, there exists a period of time where the load is maximum, which implies that the thermal bound must always be respected, which is only possible with caliber type 7.

In contrast, Figure 8 shows the voltage profiles in the 27 nodes of the balanced system, where it can be seen that the voltage value is never lower than 0.959pu, and this is the value of the voltage of node 10 in scenario 2.

Table 15. Conductor selection test system 2.

Branch	Scenario 1	Scenario 2	Scenario 3	Branch	Scenario 1	Scenario 2	Scenario 3
1	7	7	7	14	2	2	1
2	7	4	5	15	1	1	2
3	5	4	4	16	4	2	2
4	4	2	4	17	4	2	5
5	4	3	3	18	2	2	3
6	3	2	2	19	2	1	1
7	3	3	4	20	2	1	1
8	1	1	1	21	1	3	1
9	1	1	1	22	1	1	3
10	4	2	4	23	2	2	5
11	4	2	3	24	2	1	3
12	2	2	2	25	1	2	3
13	3	5	3	26	1	2	1

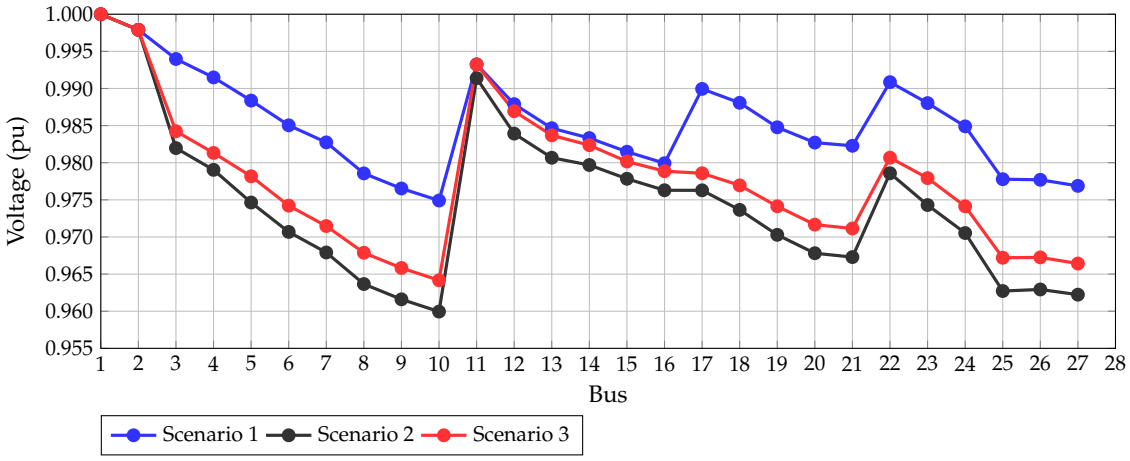

Figure 8. Voltage profile at each node for the hour of maximum demand in the three stages of case 1 of test system 2.

5.2. Results for Simulation Case 2

Here, we present all numerical results for 8- and 27-bus systems presented in Figures 4 and 5, considering all simulation scenarios with unbalanced loads.

5.2.1. Numerical Results in the 8-Bus Test System (Unbalanced)

After applying the proposed DVSA combined with the backward/forward power flow method to select the set of optimal calibers in the 8-bus system for all load scenarios, the results in Table 16 are obtained.

Table 16. Investment and operating costs in test system 2.

Scenario	Investment in Conductors (US$)	Technical Losses (US$)	Objective Function (US$)
S1	289,713	269,045.394	558,758.394
S2	273,132	117,508.615	390,640.615
S3	276,957	173,463.712	450,420.712

The results in Table 16 show that (i) *S*1 presents higher annual costs because the annual costs of the energy losses are higher when compared with the remaining simulation cases because for all periods of time, the load consumption is maximum, which also is directly associated with the increment in the investment costs of the calibers; (ii) *S*2 is the most optimist planning cases because it reduces the planning costs by approximately 30.09%

with respect to *S*1; this is attributable to the fact that during 6760 h of the year, the load is 60% of the peak case, which clearly reduces the costs of power losses by approximately 56.32% with respect to the full load case. This reduction in the cost of the annual energy losses has a direct effect on the set of calibers selected, thus reducing it by approximately US$16581 with respect to *S*1; (iii) *S*3 can be considered the more realistic simulation case because this captures the daily variations on the load profile, which have a direct effect on the annual energy loss costs and the total investment in the calibers; notably, this scenario is the intermediate simulation case with respect to the total planning case when compared with *S*1 and *S*3.

In contrast, in Table 17, the set of calibers selected for the 8-bus test feeder for the balanced case for all the simulation scenarios is presented. Note that *S*1 has calibers with higher dimensions when compared with the other two scenarios, whereas *S*2 has calibers with minimum dimensions, and *S*3 has an intermediate solution regarding the calibers, which is completely coincident with the costs of the conductors reported in Table 16. However, it is important to mention that for all the scenarios, line {1,2,3,4} has the same caliber, which implies that the thermal limit in these lines is the same and must be respected, thus selecting the same calibers for the aforementioned lines.

Table 17. Conductor selection test system 2.

Branch	Scenario 1	Scenario 2	Scenario 3
1	7	7	7
2	7	7	7
3	7	7	7
4	5	5	5
5	5	4	4
6	4	3	3
7	4	3	4

In contrast, Figure 9 shows the voltage profiles in the eight nodes and in each phase of the unbalanced system, where it can be seen that the voltage value is never lower than 0.985pu, and this value is the voltage of node 6 in phase B in scenario 2 and 3.

5.2.2. Numerical Results in the 27-Bus Test System (Unbalanced)

After applying the proposed DVSA combined with the backward/forward power flow method to select the set of optimal calibers in the 27-bus system for all load scenarios, the results in Table 18 are attained.

The results in Table 18 show that (i) *S*1 presents the higher annual costs because the annual costs of the energy losses are higher than the remaining simulation cases because for all periods of time, the load consumption is maximum, which is also directly associated with the increment in the investment costs of the calibers; (ii) *S*2 is the most optimistic planning case because it reduces the planning costs by approximately 66.55% with respect to *S*1; this is attributable to the fact that during 6760 h of the year, the load is 60% of the peak case, which clearly reduces the costs of the power losses by approximately 57.57% with respect to the full load case. This reduction in the cost of the annual energy losses has a direct effect on the set of calibers selected, thus reducing it by approximately US$94,042.5 with respect to the *S*1; (iii) *S*3 can be considered the more realistic simulation case since this captures the daily variations on the load profile, which has a direct effect on the annual energy loss costs and the total investment in the calibers; notably, this scenario is the intermediate simulation case with respect to the total planning case when compared with *S*1 and *S*3.

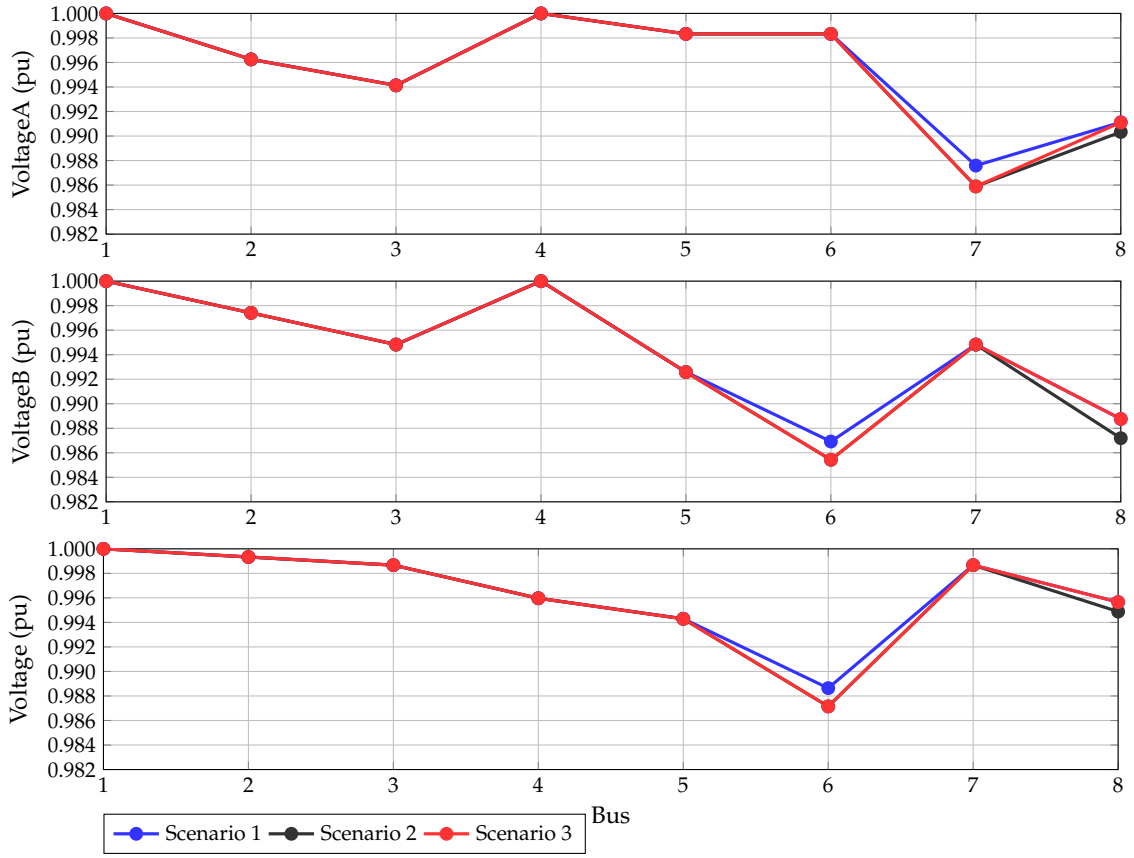

Figure 9. Voltage profile at each node for the hours of maximum demand in the three stages of case 2 of the test system 1.

Table 18. Investment and operating costs in test system 4.

Scenario	Investment in Conductors (US$)	Technical Losses (US$)	Objective Function (US$)
S1	350,392.95	257,999.185	608,392.135
S2	256,350.45	148,536.871	404,887.321
S3	265,954.80	223,894.684	489,849.484

In contrast, in Table 19, the set of calibers selected for the 27-bus test feeder with the unbalanced case for all the simulation scenarios is present. Note that *S*1 has calibers with higher dimensions in most of the lines when compared with the other two scenarios, whereas *S*2 has calibers with the minimum dimensions, and *S*3 has an intermediate solution regarding the calibers which is completely coincident with the costs of the conductors reported in Table 18. However, it is important to mention that for all scenarios, line 1 has the same caliber, which is due to the fact that in all the cases, there exists a period of time where the load is maximum, which implies that the thermal bound must always be respected, which is only possible with the caliber type 7.

In contrast, Figure 10 shows the voltage profiles in the 27 nodes and in each phase of the unbalanced system, where it can be seen that the voltage value is never lower than 0.943 pu, and this value is the voltage of node 10 in phase C in scenario 2.

Table 19. Conductor selection test system 4.

Branch	Scenario 1	Scenario 2	Scenario 3	Branch	Scenario 1	Scenario 2	Scenario 3
1	7	7	7	14	1	1	1
2	7	5	5	15	1	1	1
3	5	4	5	16	2	2	3
4	4	4	3	17	3	4	3
5	4	2	4	18	2	2	2
6	4	3	3	19	1	2	1
7	4	4	3	20	2	1	1
8	2	1	2	21	2	2	3
9	2	1	1	22	1	1	1
10	4	4	2	23	2	2	3
11	4	3	4	24	2	3	2
12	3	2	2	25	4	1	3
13	2	2	2	26	1	1	2

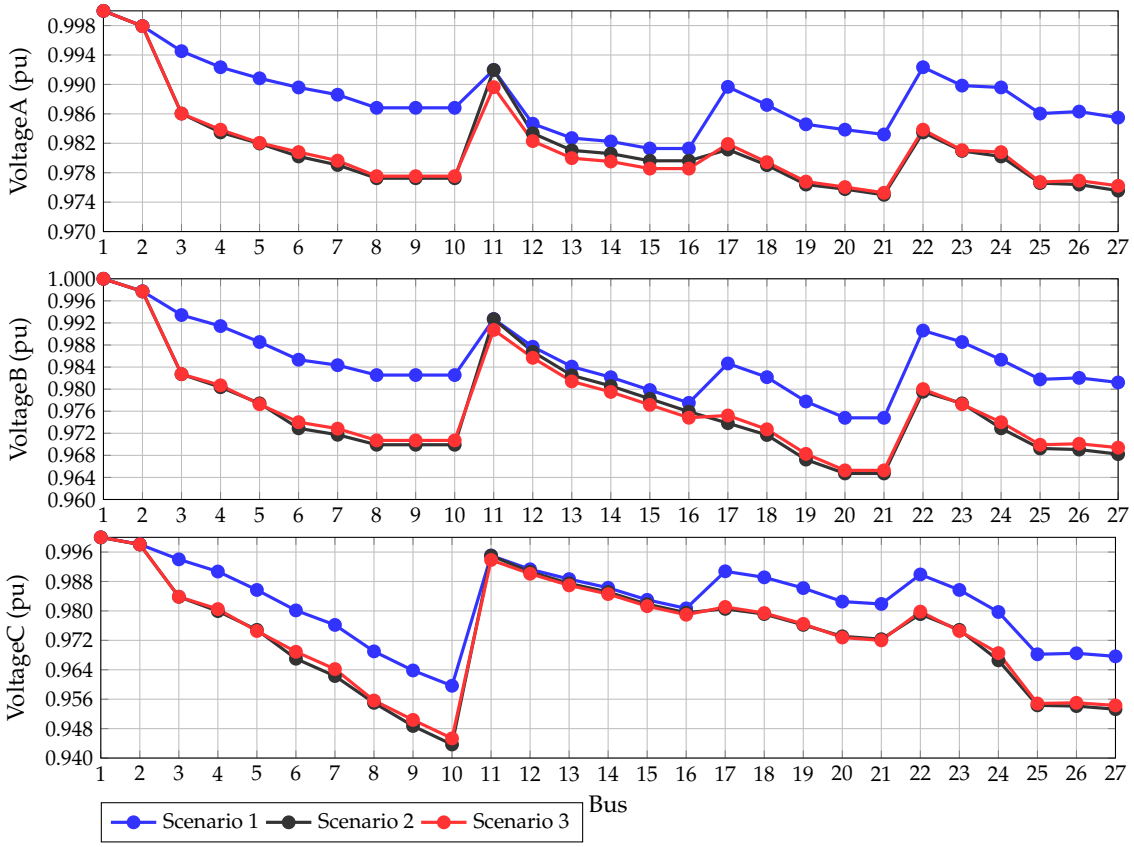

Figure 10. Voltage profile at each node for the hour of maximum demand in the three stages of case 2 of test system 2.

6. Comparative Analyses

In this section, we present a comparative study with the optimization results obtained with the proposed DVSA for the 8- and 27-bus systems and results reported in literature. For doing so, our results regarding conductors and the results provided in the literature are simulated in the backward/forward power flow approach.

6.1. Case 1 for the 8-Bus System

This section presents a comparative analysis for the 8-bus system when the loads are connected in a balanced way with purely *Y*-connection.

6.1.1. Scenario 1

Table 20 presents the results regarding the selection of the conductors with different comparative methods such as traditional genetic algorithm (TGA), Chu & Beasley genetic algorithm (CBGA), MINLP solution in the GAMS software, tabu search algorithm (TSA), and the proposed DVSA. These comparisons show the costs of the energy losses, type of conductors, and their investment costs.

Table 20. Comparative results in the 8-bus systems for the balanced load case for *S*1.

Method	Calibers	Investment in Conductors (US$)	Technical Losses (US$)	Objective Function (US$)
TGA	{6, 5, 3, 4, 4, 1, 4}	125,433	406,222.461	531,655.461
CBGA	{6, 6, 4, 4, 4, 1, 4}	143,076	373,155.965	516,231.965
MINLP	{6, 4, 4, 5, 4, 1, 2}	122,358	416,681.580	539,039.580
TSA	{6, 5, 4, 4, 4, 1, 3}	125,433	397,754.442	523,187.442
DVSA	{6, 6, 5, 5, 4, 2, 4}	163,350	345,007.959	508,357.959

The results presented in Table 20 show that (i) the most economic approach corresponds to the proposed DVSA with a total planning cost of US$508,357.959, i.e., US$7874.006 of net profit, with respect to the CBGA, which corresponds to the second better optimization method in this simulation scenario; (ii) the most expensive solution is the MINLP approach solved in the GAMS software with US$30,681.621 additional annual costs. This situation is attributable to the fact that the MINLP model is complex to solve because of the nonlinearities and non-convexities of the exact optimization model, because of which it is highly probable that the exact optimization methods may get stuck in the local optima; and (iii) the total investment on conductors is more expensive in the proposed DVSA, however, with respect to all comparative methods, which is easily observable in the final caliber solution because it is a unique solution that employs two calibers number 5; however, these additional investments are compensated for with the minimum costs of annual energy losses because the reduction in the resistance effect in some of the lines is directly proportional to the number of energy losses and their costs.

6.1.2. Scenario 2

Table 21 presents results of the second scenario, i.e., three levels in the duration load curve. In the current literature for the 8-bus system, solutions have only been reported with the TSA and the MINLP approach, which are used to compare the effectiveness of the proposed master-slave optimizer.

Table 21. Comparative results in the 8-bus system for the balanced load case for *S*2.

Method	Calibers	Investment in Conductors (US$)	Technical Losses (US$)	Objective Function (US$)
MINLP	{6, 3, 3, 4, 2, 1, 1}	96,465	201,413.772	297,878.772
TSA	{6, 4, 3, 3, 2, 1, 2}	98,877	192,127.302	291,004.302
DVSA	{6, 4, 4, 4, 3, 1, 3}	112,677	171,321.867	283,998.867

Note that the results achieved by the proposed DVSA are better than the results reached by the MINLP and the TSA methods with improvements of US$13,879.905 and US$7005.435, respectively. In addition, the calibers obtained by the DVSA include three conductors with caliber number 4, which increases its investment costs; however, this additional inversion is compensated for with important reductions in the cost of energy losses.

6.1.3. Scenario 3

In this scenario, we compare the results obtained with the proposed DVSA and the literature report using the MINLP approach considering a daily load scenario. The results of the comparison are presented in Table 22.

Table 22. Comparative results in the 8-bus systems for the balanced load case for *S*3.

Method	Calibers	Investment in Conductors (US$)	Technical Losses (US$)	Objective Function (US$)
MINLP	$\{6,4,4,4,3,1,2\}$	109,602	265,794.275	375,396.275
DVSA	$\{6,5,4,4,4,1,4\}$	129,258	236,968.262	366,226.262

In this multiperiod simulation scenario, the proposed DVSA allows a reduction of approximately 2.442% with respect to the MINLP approach. The DVSA selects four calibers of number 4 which increase the investment in conductors by approximately US$19,656 with respect to the MINLP approach; however, these additional investments in calibers imply a reduction of US$28,826.013 in the annual energy losses costs. These variations in the components of the objective function allow better performance of the DVSA when compared with the MINLP method with a net profit of US$9170.013.

Notably, no comparative analysis with different optimization methods are presented for the 27-bus system since in the specialized literature, are not reports for this test feeder as the cases analyzed in this research.

6.2. Case 2 for the 8-Bus System

In this subsection, we compare the performance of the proposed optimization method, i.e., the DVSA approach, to select calibers in the three-phase network under balanced and unbalanced load operations for all three simulation scenarios. All numerical results in the 8-bus system are reported in Table 23.

Table 23. Analysis of the 8-bus system with the DVSA approach for *Y* load connections.

Sc.	Method	Calibers	Investment in Conductors (US$)	Technical Losses (US$)	Objective Function (US$)
S1	Balanced	$\{6,6,5,5,4,2,4\}$	163,350	345,007.959	508,357.959
	Unbalanced	$\{7,7,7,5,5,4,4\}$	289,713	269,045.394	558,758.394
S2	Balanced	$\{6,4,4,4,3,1,3\}$	112,677	171,321.866	283,998.866
	Unbalanced	$\{7,7,7,5,4,3,3\}$	273,132	117,508.615	390,640.615
S3	Balanced	$\{6,5,4,4,4,1,4\}$	129,258	236,968.262	366,226.262
	Unbalanced	$\{7,7,7,5,4,3,4\}$	276,957	173,463.712	450,420.712

Considering the results reported in Table 23, we can observe that (i) for each one of the simulation scenarios, the unbalanced operation produces high increments in the final planning with increments of approximately 9.020%, 27.299%, and 18.692%, respectively; and (ii) the main effect of the unbalanced operation corresponds to the increment in the maximum caliber used, which is 7 for all the simulation cases, while in the balanced cased, the maximum number of calibers was 6. This increment in the size of the calibers produces a high increment in the investment costs of the conductors, which are not compensated for with a reduction in the energy loss costs.

6.3. Case 2 for the 27-BUS System

Here, we present the numerical performance of the proposed DVSA to select calibers in three-phase distribution networks considering balanced and unbalanced load

operations for the 27-bus system. Table 24 presents a comparative analysis for all three simulation cases.

Table 24. Analysis of the 27-bus system with the DVSA approach for Y load connections.

Sc.	Method	Calibers	Investment in Conductors (US$)	Technical Losses (US$)	Objective Function (US$)
S1	Bal.	$\left\{\begin{matrix}7,7,5,4,4,3,3,1,1,4,4,2,3,\\2,1,4,4,2,2,2,1,1,2,2,1,1\end{matrix}\right\}$	344,352.15	217,672.327	562,024.477
	Unbal.	$\left\{\begin{matrix}7,7,5,4,4,4,4,2,2,4,4,3,2,\\1,1,2,3,2,1,2,2,1,2,2,4,1\end{matrix}\right\}$	350,392.95	257,999.185	608,392.135
S2	Bal.	$\left\{\begin{matrix}7,4,4,2,3,2,3,1,1,2,2,2,5,\\2,1,2,2,2,1,1,3,1,2,1,2,2\end{matrix}\right\}$	232,566.51	155,671.759	388,238.269
	Unb	$\left\{\begin{matrix}7,5,4,4,2,3,4,1,1,4,3,2,2,\\1,1,2,4,2,2,1,2,1,2,3,1,1\end{matrix}\right\}$	256,350.45	148,536.871	404,887.321
S3	Bal.	$\left\{\begin{matrix}7,5,4,4,3,2,4,1,1,4,3,2,3,\\1,2,2,5,3,1,1,1,3,5,3,3,1\end{matrix}\right\}$	279,480.00	196,153.637	475,633.637
	Unbal.	$\left\{\begin{matrix}7,5,5,3,4,3,3,2,1,2,4,2,2,\\1,1,3,3,2,1,1,3,1,3,2,3,2\end{matrix}\right\}$	265,954.80	223,894.684	489,849.484

Results in Table 24 allow observing that as well as happened in the 8-bus system, for the 27-bus system the unbalanced load case increments the total cost of the distribution system planning about 7.621% for the $S1$, 4.112% for the $S2$, and 2.902% for the $S3$.

6.4. Analysis of the S1 for Three-Phase Grids with Loads Connected in Δ and Y

The type of load connection in distribution networks can have incidence in the final planning solution for the three-phase network since the amount of power losses depends on the load configuration, i.e., Δ- and Y-connections. Numerical results for both test feeders are presented in Tables 25 and 26.

Table 25. Comparative analysis for the 8-bus system with loads with Δ- and Y-connections.

Scenario	Method	Branch	Investment in Conductors (US$)	Technical Losses (US$)	Objective Function (US$)
S1	Balanced (Y)	$\{6,6,5,5,4,2,4\}$	163,350	345,007.959	508,357.959
	Balanced (Δ)	$\{6,6,5,5,4,2,4\}$	163,350	345,007.959	508,357.959
	Unbalanced (Y)	$\{7,7,7,5,5,4,4\}$	289,713	269,045.394	558,758.394
	Unbalanced (Δ)	$\{7,7,7,5,5,4,4\}$	289,713	225,328.908	515,041.908

Table 26. Comparative analysis for the 27-bus system with loads with Δ- and Y-connections.

Sc.	Method	Calibers	Investment in Conductors (US$)	Technical Losses (US$)	Objective Function (US$)
S1	Bal. (Y)	$\left\{\begin{matrix}7,7,5,4,4,3,3,1,1,4,4,2,3,\\2,1,4,4,2,2,2,1,1,2,2,1,1\end{matrix}\right\}$	344,352.150	217,672.327	562,024.477
	Bal. (Δ)	$\left\{\begin{matrix}7,7,4,4,3,2,3,1,1,4,3,3,1,\\1,1,3,2,2,2,1,2,1,2,2,3,1\end{matrix}\right\}$	323,408.430	238,750.389	562,158.819
	Unbal. (Y)	$\left\{\begin{matrix}7,7,5,4,4,4,4,2,2,4,4,3,2,\\1,1,2,3,2,1,2,2,1,2,2,4,1\end{matrix}\right\}$	350,392.950	257,999.185	608,392.135
	Unbal. (Δ)	$\left\{\begin{matrix}7,7,5,4,4,3,4,1,2,4,3,4,3,\\2,1,4,2,3,1,1,1,1,1,2,4,2\end{matrix}\right\}$	351,535.500	235,055.525	586,591.025

In the case of the 8-bus system, we can observe that the optimal plan regarding the calibers for the balanced and unbalanced load cases are the same with inversions of

US$163,350 and US$289,713; however, regarding the cost of energy losses, there are important differences in the unbalanced load case between the Y-connections when compared with the Δ-connections; making the Y-connection case more expensive with a net increment of US$43,716.486.

In the case of the 27-bus system, we can observe that the Y-connection is, in general, more expensive than the Δ-connection case; however, it is no possible to generalize this result with respect to the investment in conductors and the total energy loss costs because for the balanced load case, the cost of calibers for the Y-connection is US$20,943.72 higher than that for the Δ-connection case. However, in the unbalanced load scenario, the Δ-connection case is US$1142.550 higher than the Y-connection case. In addition, notably, for the 27-bus system, in general, for the unbalanced load cases, the final planning project is more expensive than the balanced case with differences of US$46,367.658 and US$24,432.206 for Y- and Δ-connections, respectively.

6.5. Complementary Analysis

This subsection explores three additional aspects related with the problem of the optimal selection of the calibers of conductors in three-phase networks by applying the DVSA. These aspects are as follows: (i) the effect of the renewable generation; (ii) the general processing time behavior of the proposed optimization method; and (iii) the convergence behavior of the DVSA as a function of the number of iterations. Each one of these aspects is presented below.

Analysis of the Effect of the Renewable Generation in the Final Optimization Plane

In this simulation scenario, we consider the effect of the renewable energy in the optimal selection of calibers for three-phase distribution networks. For doing so, we consider the S3 in the 27-bus system. For this test feeder, a wind generation source is connected at node 13 with a nominal rate of 3000 kW, and a photovoltaic source is assigned at node 7 with a generation capacity of 3500 kW. Figure 11 depicts the normalized generation curve considered for each generation source; however, to guarantee verification of our results, in Table 27, the generation values for each time period are listed.

Table 27. Renewable behavior.

Time (h)	Solar (%)	Wind (%)	Time (h)	Solar (%)	Wind (%)
1	0	0.633118295	13	0.924486326	0.972218577
2	0	0.607259323	14	0.982041153	0.981135531
3	0	0.605557422	15	0.829407079	0.991393173
4	0	0.684246423	16	0.733063295	1.0
5	0	0.783719339	17	0.501133849	0.987258076
6	0	0.790557706	18	0.177117518	0.929542167
7	0	0.744958950	19	0	0.791155379
8	0.039123365	0.769603567	20	0.000333920	0.708839248
9	0.065587179	0.826492212	21	0	0.712881960
10	0.236870796	0.876523598	22	0	0.719897641
11	0.455017818	0.931213527	23	0	0.703007456
12	0.726440265	0.965504834	24	0	0.687238555

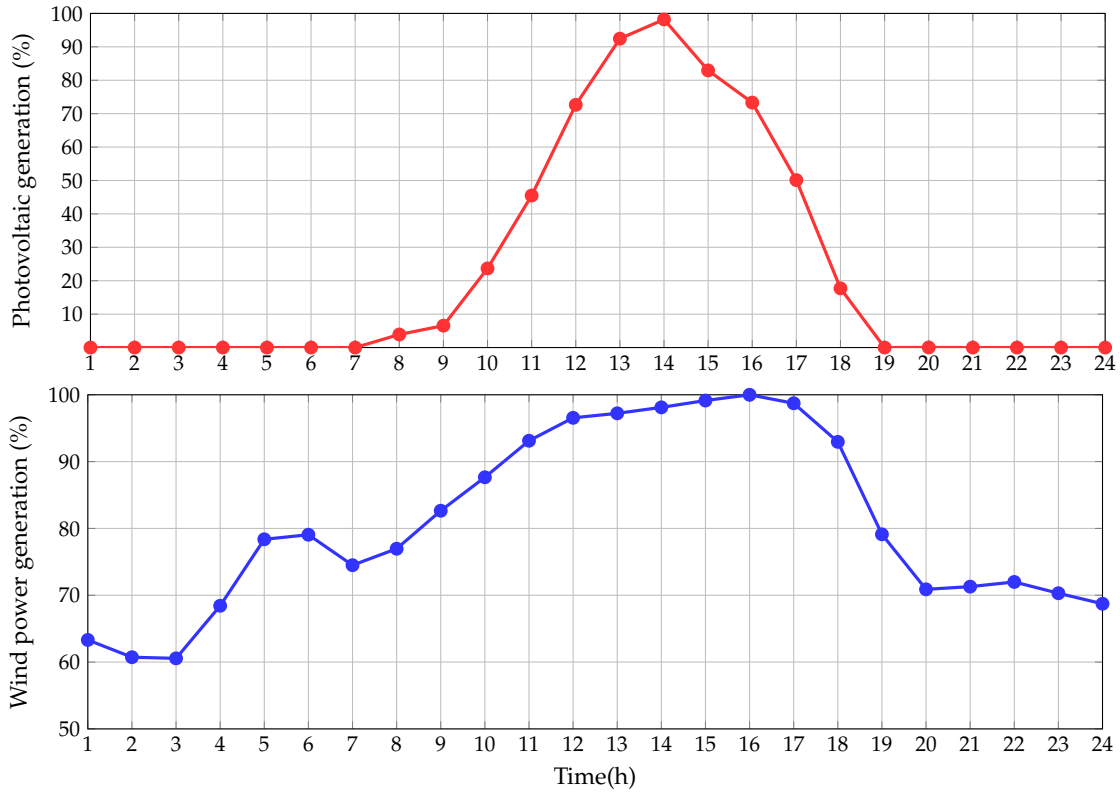

Figure 11. Renewable behavior.

Table 28 presents the numerical results of the 27-bus system with unbalanced operated condition with distributed generation.

Table 28. Analysis of the 27-bus system with renewable energy.

Sc.	Method	Calibers	Investment in Conductors (US$)	Technical Losses (US$)	Objective Function (US$)
S3	Unbal.	$\begin{Bmatrix} 7,5,5,3,4,3,3,2,1,2,4,2,2, \\ 1,1,3,3,2,1,1,3,1,3,2,3,2 \end{Bmatrix}$	265,954.800	223,894.684	489,849.484
S3	Unbal. renew.	$\begin{Bmatrix} 7,6,6,3,3,4,3,3,1,3,1,1,3, \\ 1,1,2,3,1,2,1,1,2,3,2,1,1 \end{Bmatrix}$	276,452.940	165,278.066	441,731.006

Notably, the investment in conductors increases by approximately US$10,498.14; however, this additional investment reduces the resistance value in some lines (low power losses) which is traduced in a net reduction in the cost of the energy losses by approximately US$58,616.618. With the aforementioned variations in the investment and operating costs, the expected objective was reduced by approximately US$48,118.478, which implies a reduction of approximately 9.76% with respect to the case without renewables.

6.6. Computational Effort

One of the main aspects in the analysis and comparison of different optimization methods applied to power engineering problems corresponds to the total processing time taken by each method. Here, we present the total processing time of the proposed DVSA for each one of the test feeder and simulation cases, respectively; these values are listed in Table 29.

Table 29. Processing times expended by the DVSA in each test feeder and simulation case.

Sc.	8-bus bal. (s)	8-bus Unbal. (s)	27-bus bal. (s)	27-bus Unbal. (s)	27-bus Renew. (s)
S1	15.149	33.157	89.842	90.487	—
S2	40.463	45.573	203.122	215.280	—
S3	277.998	307.762	1557.902	1539.686	1717.367

The processing times reported in Table 29 show that (i) in all the test feeders and simulation cases, the unbalanced operation of the network increases the required processing time to find a solution for the optimization problem. This behavior is because the unbalanced operation of the network needs additional iterations to solve the power flow problem at the exact objective function evaluation, which finally affects the global processing time expended by the DVSA to solve it; (ii) the third simulation scenario takes more than 300 s in the 8-bus system and 1500 s in the 27-bus system to solve the optimization problem; however, in general terms, this behavior is expected because S3 includes 24 periods of time to be evaluated in the power flow, whereas S1 and S2 only need 1 and 3 periods to be solved, respectively; in addition, the total processing time is directly influenced by the size of the solution space, which is approximately 7^7 and 7^26 for both test feeders, which is 823,543 (i.e., thousands combinations) for the 8-bus system, and 9.3874803×10^{21} (billion combinations) in the 27-bus system, respectively; and (iii) the behavior of the renewable energy case in the 27-bus system increases by approximately 177.681 s compared with the simulation case without renewables. This time increment is caused by the additional time required to introduce wind and photovoltaic generation in the power flow evaluations; however, this is also negligible due to the size of the solution space explored, i.e., 9.3874803×10^{21}.

6.7. Graphic Convergence Behavior

To illustrate the convergence behavior of the proposed DVSA to solve the problem of the optimal selection of calibers in three-phase distribution networks, Figure 12 shows the evolution of the objective function value as a function of the number of iterations in the 8-bus system with balanced loads.

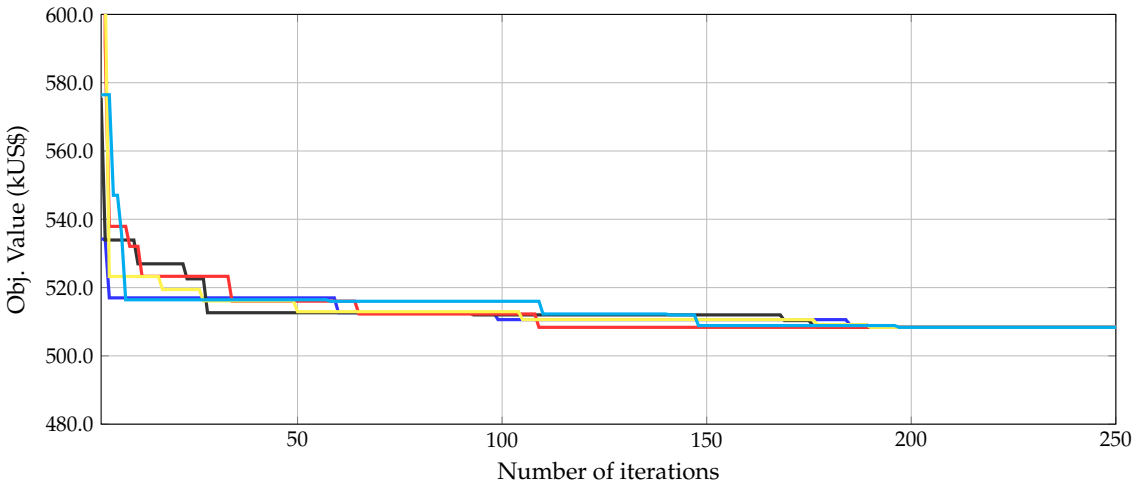

Figure 12. Behavior of the objective function value for the 8-bus system with balanced loads.

This graphic shows that after 200 iterations, DVSA finds an objective function that is stabilized at the final value, which was proved with 5 different consecutive simulations. This behavior of the objective function value confirms the effectiveness and robustness of the DVSA to solve complex problems with discrete variables using hyper-spheres to explore

and exploit the solution space considering a variable radius to balance the exploration and exploitation stages.

7. Conclusions

The problem of optimal selection of calibers of conductors in three-phase distribution networks with balanced and unbalanced load cases and three different curves regarding the annual load consumption was addressed in this study from the viewpoint of master-slave optimization. In the master stage, the discrete version of the vortex search algorithm was employed to define the subset of calibers to be installed in the network with their corresponding investment costs; the slave stage was entrusted with evaluating the costs of the annual energy loss costs by employing a classical backward/forward optimization approach. Numerical validations in the 8- and 27-bus systems demonstrate that the proposed DVSA attained the best optimal solutions when compared with different optimization methods reported in the literature such as traditional and Chu & Beasley genetic algorithms, tabu search algorithms, and the exact MINLP methods.

The third simulation scenario where a daily load curve is used to determine the optimal set of calibers in the three-phase networks presents a more realistic simulation scenario when compared with the peak load case (first simulation scenario) and the load duration curve with three periods (second simulation scenario) because in both test feeders, their solutions are in the intermediates of the $S1$ and $S2$. This was an expected result because if the annual demand curve is well characterized, then the costs of the final distribution system plan are nearest to the real operation case. With these results, we concluded that $S1$ will cause over-inversions, while $S2$ will cause under-inversions in conductors that can affect the distribution company finances.

The effect of the inclusion of renewable generation with photovoltaic and wind technologies was explored in the 27-bus system. Numerical results demonstrated that the final cost of the plan is reduced by approximately 9.76% with respect to the case without renewables. This behavior of the objective function was allowed by an increment of approximately US$10,498.14 in the investment in conductors, which produced a reduction in the energy loss costs by approximately US$58,616.618. The difference between both values have produced a net profit of US$48,118.478 in favor of the integration of renewables in three-phase networks.

Analysis with balanced and unbalanced load cases including Δ- and Y-connections in the loads demonstrated that the costs of the final distribution system planning project will have important variations, and the costs will be more than US$50,000 and US$6000 for the Y- and Δ- connections in the 8-bus system, respectively; and more than US$46,000 and US$624,000 for the Y- and Δ-connections in the 27-bus system, respectively.

The nonlinear behavior that exhibits the final costs of the distribution system planning projects for the 8- and 27-bus systems allows us to propose the following future works: (i) to extend the proposed codification of the DVSA to solve simultaneously the problem of the phase-balancing and the selection of the conductor size problems in three-phase networks in a unique optimization stage to reduce the final costs of the distribution system planning project as possible; (ii) to include the effect of renewable energy resources connected in some demand nodes in the optimal selection of calibers in three-phase networks using a three-phase optimal power-flow formulation; and (iii) to propose an optimization approach that allows us to obtain the optimal Pareto front between the investment costs in conductors and the annual energy loss costs that will exhibit a clearly multi-objective compromise.

Author Contributions: Conceptualization, J.F.M.-G.; N.A.M.-G.; O.D.M.; and J.A.A.-V.; Methodology, J.F.M.-G.; N.A.M.-G.; O.D.M.; and J.A.A.-V.; Investigation, J.F.M.-G.; N.A.M.-G.; O.D.M.; and J.A.A.-V.; Writing—review and editing, J.F.M.-G.; N.A.M.-G.; O.D.M.; and J.A.A.-V. All authors have read and agreed to the published version of the manuscript.

Funding: This work was supported in part by the Centro de Investigación y Desarrollo Científico de la Universidad Distrital Francisco José de Caldas under grant 1643-12-2020 associated with

the project: "Desarrollo de una metodología de optimización para la gestión óptima de recursos energéticos distribuidos en redes de distribución de energía eléctrica." and in part by the Dirección de Investigaciones de la Universidad Tecnológica de Bolívar under grant PS2020002 associated with the project: "Ubicación óptima de bancos de capacitores de paso fijo en redes eléctricas de distribución para reducción de costos y pérdidas de energía: Aplicación de métodos exactos y metaheurísticos."

Data Availability Statement: No new data were created or analyzed in this study. Data sharing is not applicable to this article.

Acknowledgments: This work has been derived from the undergraduate project:"Selección óptima de conductores en redes de distribución trifásicas utilizando una versión discreta del algoritmo de búsqueda por vórtices" presented by the students John Fernando Martínez-Gil and Nicolas Alejandro Moyano-García to the Electrical Engineering Program of the Engineering Faculty at Universidad Distrital Francisco José de Caldas as a partial requirement for the Bachelor in Electrical Engineering.

Conflicts of Interest: The authors declare no conflicts of interest.

Nomenclature

C_{loss}	Annual costs of the energy losses (US$/year).
C_{inv}	Cost of the inversion in calibers installed in all the distribution lines (US$).
C_{pen}	Cost of the penalization for constraints violations (US$).
C_p	Average energy cost (US$/kWh).
h	Sub-index with time intervals.
$\phi_{h,i}^{p}$	Voltage angle at node i for phase p in the period of time h (rad).
$\phi_{h,j}^{q}$	Voltage angle at node j for phase q in the period of time h (rad).
$\phi_{h,ij}^{pq}$	Admittance angle that relates nodes i and j and phases p and q (rad).
C_{km}	Costs of the conductor installed in route km with caliber type c (US$/km).
L_{km}	Length of the route that connects nodes k and m (km).
λ_{km}^{c}	Binary variable that defines if the caliber type c is assigned to the route km.
z	Objective function value (US$).
Y_{ij}^{pq}	Admittance magnitude that relates nodes i and j and phases p and q (S).
km	Route that connects nodes k and m.
i, j	Sub-index associated with nodes i and j.
p, q	Sub-index associated with phases.
Δ_h	Period of time associated with power-flow evaluation (h).
$P_{g_{i,h}}^{p}$	Active power generation at node i for phase p at the period of time h (W).
$Q_{g_{i,h}}^{p}$	Reactive power generation at node i for phase p at the period of time h (var).
$Q_{d_{i,h}}^{p}$	Active power demand at node i for phase p at the period of time h (W).
$Q_{d_{i,h}}^{p}$	Reactive power demand at node i for phase p at the period of time h (var).
$I_{km,h}^{p}$	Magnitude of the current flow in the route km in the period of time h for the phase p (A).
$I_c^{\max}$	Maximum thermal current for a conductor with caliber type c (A).
$V_i^{\min}$	Minimum regulation voltage allowed for the node i (V).
$V_i^{\max}$	Maximum regulation voltage allowed for the node i (V).
$V_{i,h}^{p}$	Voltage at phase p for time interval h at node i (V).
Ω_L	Set containing all lines of the distribution system.
Ω_h	Set containing all load duration periods.
Ω_p	Set containing all phases of the system.
Ω_b	Set containing all nodes of the distribution system.
c	Sub-index associated with the calibers of conductors.

References

1. Montoya, O.D.; Gil-González, W.; Hernández, J.C. Efficient Operative Cost Reduction in Distribution Grids Considering the Optimal Placement and Sizing of D-STATCOMs Using a Discrete-Continuous VSA. *Appl. Sci.* **2021**, *11*, 2175. [CrossRef]
2. Fatima, S.; Püvi, V.; Arshad, A.; Pourakbari-Kasmaei, M.; Lehtonen, M. Comparison of Economical and Technical Photovoltaic Hosting Capacity Limits in Distribution Networks. *Energies* **2021**, *14*, 2405. [CrossRef]
3. Sorrentino, E.; Gupta, N.G. Summary of useful concepts about the coordination of directional overcurrent protections. *CSEE J. Power Energy Syst.* **2019**. [CrossRef]
4. Paz, M.C.R.; Ferraz, R.G.; Bretas, A.S.; Leborgne, R.C. System unbalance and fault impedance effect on faulted distribution networks. *Comput. Math. Appl.* **2010**, *60*, 1105–1114. [CrossRef]

5. Cortés-Caicedo, B.; Avellaneda-Gómez, L.S.; Montoya, O.D.; Alvarado-Barrios, L.; Chamorro, H.R. Application of the Vortex Search Algorithm to the Phase-Balancing Problem in Distribution Systems. *Energies* **2021**, *14*, 1282. [CrossRef]
6. Lavorato, M.; Franco, J.F.; Rider, M.J.; Romero, R. Imposing Radiality Constraints in Distribution System Optimization Problems. *IEEE Trans. Power Syst.* **2012**, *27*, 172–180. [CrossRef]
7. Montoya, O.D.; Grajales, A.; Hincapié, R.A.; Granada, M. A new approach to solve the distribution system planning problem considering automatic reclosers. *Ingeniare Revista Chilena de Ingeniería* **2017**, *25*, 415–429. [CrossRef]
8. Wang, Z.; Liu, H.; Yu, D.; Wang, X.; Song, H. A practical approach to the conductor size selection in planning radial distribution systems. *IEEE Trans. Power Deliv.* **2000**, *15*, 350–354. [CrossRef]
9. Zhao, Z.; Mutale, J. Optimal Conductor Size Selection in Distribution Networks with High Penetration of Distributed Generation Using Adaptive Genetic Algorithm. *Energies* **2019**, *12*, 2065. [CrossRef]
10. Montoya, O.; Grajales, A.; Hincapié, R. Optimal selection of conductors in distribution systems using tabu search algorithm. *Ingeniare Revista Chilena de Ingeniería* **2018**, *26*, 283–295. [CrossRef]
11. Ismael, S.M.; Aleem, S.H.E.A.; Abdelaziz, A.Y. Optimal selection of conductors in Egyptian radial distribution systems using sine-cosine optimization algorithm. In Proceedings of the 2017 Nineteenth International Middle East Power Systems Conference (MEPCON), Hibbingum, Egypt, 19–21 December 2017; IEEE: Piscataway, NJ, USA, 2017. [CrossRef]
12. Joshi, D.; Burada, S.; Mistry, K.D. Distribution system planning with optimal conductor selection. In Proceedings of the 2017 Recent Developments in Control, Automation & Power Engineering (RDCAPE), Noida, India, 26–27 October 2017; IEEE: Piscataway, NJ, USA, 2017. [CrossRef]
13. Ismael, S.M.; Aleem, S.H.E.A.; Abdelaziz, A.Y.; Zobaa, A.F. Practical Considerations for Optimal Conductor Reinforcement and Hosting Capacity Enhancement in Radial Distribution Systems. *IEEE Access* **2018**, *6*, 27268–27277. [CrossRef]
14. Mandal, S.; Pahwa, A. Optimal selection of conductors for distribution feeders. *IEEE Trans. Power Syst.* **2002**, *17*, 192–197. [CrossRef]
15. Falaghi, H.; Singh, C. Optimal Conductor Size Selection in Distribution Systems with Wind Power Generation. In *Green Energy and Technology*; Springer: Berlin/Heidelberg, Germany, 2010; pp. 25–51. [CrossRef]
16. Legha, M.; Javaheri, H.; Legha, M. Optimal Conductor Selection in Radial Distribution Systems for Productivity Improvement Using Genetic Algorithm. *Iraqi J. Electr. Electron. Eng.* **2013**, *9*, 29–35. [CrossRef]
17. Rao, R.S.; Satish, K.; Narasimham, S.V.L. Optimal Conductor Size Selection in Distribution Systems Using the Harmony Search Algorithm with a Differential Operator. *Electr. Power Compon. Syst.* **2011**, *40*, 41–56. [CrossRef]
18. Lopez, L.; Hincapié, R.A.; Gallego, R.A. Planeamiento multi-objetivo de sistemas de distribución usando un algoritmo evolutivo NSGA-II. *Revista Escuela de Ingeniería de Antioquía* **2011**, *15*, 141–151.
19. Khalil, T.M.; Gorpinich, A.V. Optimal conductor selection and capacitor placement for loss reduction of radial distribution systems by selective particle swarm optimization. In Proceedings of the 2012 Seventh International Conference on Computer Engineering & Systems (ICCES), Cairo, Egypt, 27–29 November 2012; IEEE: Piscataway, NJ, USA 2012. [CrossRef]
20. Legha, M.M.; Noormohamadi, H.; Barkhori, A. Optimal conductor selection in radial distribution using bacterial foraging algorithm and comparison with ICA method. *WALIA J.* **2015**. *31*, 37–43.
21. Abdelaziz, A.Y.; Fathy, A. A novel approach based on crow search algorithm for optimal selection of conductor size in radial distribution networks. *Eng. Sci. Technol. Int. J.* **2017**, *20*, 391–402. [CrossRef]
22. Hassen, S.Z.S.; Jahmeerbacus, M.I. Customer Loss Allocation Reduction Using Optimal Conductor Selection in Electrical Distribution System. In *Emerging Trends in Electrical, Electronic and Communications Engineering*; Springer: Singapore, 2017; Volume 416, pp. 372–379. [CrossRef]
23. Montoya, O.D.; Garces, A.; Castro, C.A. Optimal Conductor Size Selection in Radial Distribution Networks Using a Mixed-Integer Non-Linear Programming Formulation. *IEEE Latin Am. Trans.* **2018**, *16*, 2213–2220. [CrossRef]
24. Montoya, O.D.; Gil-González, W.; Grisales-Noreña, L.F. On the mathematical modeling for optimal selecting of calibers of conductors in DC radial distribution networks: An MINLP approach. *Electr. Power Syst. Res.* **2021**, *194*, 107072. [CrossRef]
25. Ismael, S.M.; Aleem, S.H.E.A.; Abdelaziz, A.Y. Optimal conductor selection in radial distribution systems using whale optimization algorithm. *J. Eng. Sci. Technol.* **2017**, *14*, 87–107.
26. Kumari, M.; Singh, V.R.; Ranjan, R. Optimal selection of conductor in RDS considering weather condition. In Proceedings of the 2018 International Conference on Computing, Power and Communication Technologies, GUCON 2018, New Delhi, India, 28–29 September 2018; pp. 647–651. [CrossRef]
27. Mohanty, S.; Kasturi, K.; Nayak, M.R. Application of ER-WCA to Determine Conductor Size for Performance Improvement in Distribution System. In Proceedings of the 2021 International Conference on Advances in Electrical, Computing, Communication and Sustainable Technologies (ICAECT), Bhilai, India, 19–20 February 2021, pp. 1–5. [CrossRef]
28. Paz-Rodríguez, A.; Castro-Ordoñez, J.F.; Montoya, O.D.; Giral-Ramírez, D.A. Optimal Integration of Photovoltaic Sources in Distribution Networks for Daily Energy Losses Minimization Using the Vortex Search Algorithm. *Appl. Sci.* **2021**, *11*, 4418. [CrossRef]
29. Dogan, B.; Yuksel, A. Analog filter group delay optimization using the Vortex Search algorithm. In Proceedings of the 2015 23nd Signal Processing and Communications Applications Conference (SIU), Malatya, Turkey, 16–19 May 2015. [CrossRef]
30. Serna-Suárez, I.D. A Convex Approximation for Optimal DER Scheduling on Unbal-anced Power Distribution Networks. *DYNA* **2019**, *86*, 281–291. [CrossRef]

31. Wang, C.; Liu, P.; Zhang, T.; Sun, J. The Adaptive Vortex Search Algorithm of Optimal Path Planning for Forest Fire Rescue UAV. In Proceedings of the 2018 IEEE 3rd Advanced Information Technology, Electronic and Automation Control Conference, IAEAC 2018, Chongqing, China, 12–14 October 2018; pp. 400–403. [CrossRef]
32. Montoya, O.D.; Gil-Gonzalez, W.; Grisales-Norena, L.F. Vortex Search Algorithm for Optimal Power Flow Analysis in DC Resistive Networks with CPLs. *IEEE Trans. Circ. Syst. II Express Briefs* **2020**, *67*, 1439–1443. [CrossRef]
33. Shen, T.; Li, Y.; Xiang, J. A graph-based power flow method for balanced distribution systems. *Energies* **2018**, *11*, 511. [CrossRef]
34. Castilho Neto, J.; Cossi, A.M. Alocação de Cabos em Redes de Distribuição de Energia Elétrica de Média Tensão (MT) Utilizando Algoritmo Chu-Beasley. In Proceedings of the Simpósio Brasileiro de Sistemas Eletricos (SBSE), Foz do Iguacu, Brasil, 22–25 April 2014; pp. 1–6.
35. Soroudi, A. Multi-Period Optimal Power Flow. In *Alireza Soroudi Power System Optimization Modeling in GAMS*; Springer: Singapore, 2019; Chapter 6, pp. 2017–2020.